# The Intrinsically Disordered Region of ExbD is Required for Signal Transduction.

Dale R. Kopp[1] and Kathleen Postle[*]

Running title: *ExbD-mediated signal transduction*

**Keywords: TonB, ExbD, intrinsic disorder, conserved binding motif, energy transduction**

[1]Department of Biochemistry and Molecular Biology, The Pennsylvania State University, University Park, PA, 16802, USA

* Correspondence:

Kathleen Postle, Department of Biochemistry and Molecular Biology, The Pennsylvania State University, University Park, PA 16802, USA. email: postle@psu.edu, Ph. 1-814-863-7568, Fx. 1-814-863-7024

**ABSTRACT:**

The TonB system actively transports vital nutrients across the unenergized outer membranes of the majority of Gram-negative bacteria. In this system, integral membrane proteins ExbB, ExbD, and TonB work together to transduce the protonmotive force (PMF) of the inner membrane to customized active transporters in the outer membrane by direct and cyclic binding of TonB to the transporters. A PMF-dependent TonB-ExbD interaction is prevented by 10-residue deletions within a periplasmic disordered domain of ExbD adjacent to the cytoplasmic membrane. Here we explored the function of the ExbD disordered domain in more detail. *In vivo* photo-cross-linking through sequential pBpa substitutions in the ExbD disordered domain captured five different ExbD complexes, some of which had been previously detected using in vivo formaldehyde crosslinking, a technique that lacks the residue-specific information that can be achieved through photo-cross-linking: 2 ExbB-ExbD heterodimers (one of which had not been detected previously), previously detected ExbD homodimers, previously detected PMF-dependent ExbD-TonB heterodimers, and for the first time, a predicted, ExbD-TonB PMF-*in*dependent interaction. The fact that multiple complexes were captured by the same pBpa substitution indicated the dynamic nature of ExbD interactions as the energy transduction cycle proceeded in vivo. In this study, we also discovered that a conserved motif, (V45, V47, L49, P50), within the disordered domain was required for signal transduction to TonB and to the C-terminal domain of ExbD and was the source of its essentiality.

**Importance:**

The TonB system is a virulence factor for many Gram-negative pathogens including E-S-K-A-P-E pathogenic species *Klebsiella pneumoniae*, *Acinetobacter baumannii*, *and Pseudomonas aeruginosa*. Because the majority of protein-protein interactions in the TonB system occur in the periplasm, it is an appealing target for novel antibiotics. Understanding the molecular mechanism of the TonB system will provide valuable information for design of potential inhibitors targeting the system.

68 **INTRODUCTION:**

69

70 The TonB system is required for most Gram-negative bacteria to acquire vital nutrients
71 such iron, vitamin $B_{12}$, nickel, cobalt, copper, heme, maltodextrin, and sucrose across their
72 outer-membrane barriers and is major virulence factor in many pathogenic Gram-negative
73 bacteria (1, 2). Under iron-limiting conditions, such as the human serum, Gram-negative
74 bacteria secrete iron-chelating compounds called siderophores that capture the iron with high
75 affinity (3). However, because iron-siderophore complexes are too large, too scarce, and too
76 important to passively diffuse through the outer-membrane porins, they require customized 22-
77 stranded beta-barrel transporters called TonB-dependent transporters (TBDTs) to transition
78 across the outer membrane (4, 5).

79 After the siderophore captures an iron atom extracellularly, the iron-siderophore
80 complex binds to a TDBT with sub-nanomolar affinity, causing the ligand-loaded TBDT to
81 signal on its periplasmic face that ligand is bound (6-9). Energy is required to release the iron-
82 siderophore from the TBDT (10). Because the outer membrane and periplasmic space lack a
83 sufficient energy source, Gram-negative bacteria transduce the energy from the cytoplasmic
84 membrane proton motive force (PMF) to the TBDTs using the three known integral cytoplasmic
85 membrane proteins of the TonB system--ExbB, ExbD, and TonB (11, 12).

86 In *Escherichia coli* K-12, there are six TBDTs that transport various sources of iron and
87 one TBDT that transports vitamin B12. With a cellular ratio of 7 ExbB: 2 ExbD: 1 TonB, ExbB
88 and ExbD harvest PMF and transmit it to TonB by a largely unknown mechanism (13). ExbB
89 has three transmembrane domains (TMDs) with the majority of the protein residing in the
90 cytoplasm [Fig. 1, (14, 15)]. In contrast, ExbD and TonB are anchored by single N-terminal
91 TMDs with the bulk of their residues occupying the periplasm (16, 17). ExbB, ExbD, and TonB
92 also share homology through their TMDs with proteins TolQ, TolR, and TolA of the Tol system

93 (respectively), which is important for outer membrane integrity and cell division (18, 19). Both
94 systems are energized by PMF, suggesting that they have a common means of PMF utilization
95 that plays out as different roles in cell physiology due to different protein contacts made by
96 their soluble domains (20, 21).

97 The TBDTs greatly outnumber the molecules of TonB in a cell, leading to competition
98 between TBDTs for "energized" TonB (13, 22). TonB must thus undergo a cyclic pattern of
99 binding and release from TBDT to TBDT, referred to as the TonB energization cycle (6, 23,
100 24). TonB binds to TBDTs both *in vitro* and *in vivo* whether or not it is "energized", and
101 therefore, it must be correctly configured during an energy transduction cycle to enable
102 productive interaction with the TBDT (24-28). Both ExbB and ExbD are required to correctly
103 configure TonB to energize active transport across the outer membrane--ExbB indirectly, and
104 ExbD directly (15, 29, 30).

105 ExbB serves as a scaffolding protein for ExbD and TonB assembly, without which they
106 are both proteolytically unstable, and mediates ExbD-TonB interactions (15, 31-33). ExbD-
107 TonB interactions, or lack thereof, define our model for the initial Stages of the TonB
108 energization cycle (24, 34). In Stage I, ExbD and TonB homodimers exist in separate
109 complexes with ExbB homotetramers, but do not interact. To transition to Stage II, ExbB
110 tetramers bring ExbD and TonB homodimers together in a single complex without a
111 requirement for PMF. The PMF-*in*dependent ExbD-TonB interaction has only been detected
112 indirectly by ExbD-mediated protection of the N-terminal ~155 residues of TonB from
113 exogenously added proteinase K in spheroplasts that lack PMF (6, 15, 35). In the subsequent
114 presence of PMF, Stage III, the ExbD and TonB homodimers swap partners to form ExbD-
115 TonB heterodimers. Only in this Stage can the PMF-dependent ExbD-TonB interaction can be
116 captured by formaldehyde cross-linking *in vivo* (29). The only TMD among the cytoplasmic

117 membrane proteins of ExbB, ExbD, and TonB that can participate in response to PMF is the
118 ExbD TMD, with its D25 residue (15, 29, 36).

119 ExbD has five structurally distinct domains: a cytoplasmically localized N-terminus
120 (residues 1-22), a predicted TMD (residues 23-43), a disordered periplasmic domain [44-63], a
121 structured periplasmic domain (residues 64-133) and a flexible C-terminus (residues 134-141)
122 (37). Experiments using *in vivo* disulfide cross-linking of engineered Cys residues in the ExbD
123 and TonB distal periplasmic domains are consistent with the three-Stage model. The same
124 ExbD residues in the region of 92-121 that form a homodimeric interface are almost the exact
125 same residues that form ExbD-TonB heterodimers through the TonB periplasmic domain (38).
126 Also, in a PMF-unresponsive ExbD mutant, ExbD (D25N), ExbD-TonB disulfide cross-links are
127 either absent or significantly reduced (39).

128 A 10 residue-deletion scanning mutagenesis of ExbD reveals that deletions within ExbD
129 periplasmic residues 62-141 stall TonB energization in Stage I, whereas deletions largely
130 encompassing the disordered domain of ExbD [42-61] stall TonB energization in Stage II,
131 unable to proceed to Stage III (35). However, the mechanistic details of how the ExbD
132 disordered domain participates in energy transduction have remained unclear.

133 Here we discovered that a novel motif, ΨXΨXLP (Ψ = hydrophobic-branched residues;
134 X = non-hydrophobic residues) encompassing ExbD residues V45, V47, L49 and P50 and
135 located adjacent to the ExbD TMD, is essential for ExbD signal transduction to its periplasmic
136 C-terminus and to TonB. This motif within the disordered domain of ExbD is required for the
137 transition from Stage II to Stage III and could account for crosstalk between the TonB and Tol
138 systems because it is conserved in TolR. As might be predicted from its lack of structure, the
139 disordered domain is highly dynamic, making contacts with TonB, another ExbD and two
140 different contacts with ExbB. With respect to TonB contacts, the disordered domain forms the

141 PMF-dependent complex previously visualized by formaldehyde cross-linking. Importantly, it
142 also forms the long-predicted PMF-*in*dependent complex between ExbD and TonB, visualized
143 for the first time without requiring collapse of PMF, thus indicating it is part of the normal
144 energy transduction cycle. This study defines the role of the ExbD disordered domain and
145 makes clear the dynamic character of protein-protein interactions that occur during TonB-
146 dependent energy transduction.
147
148 **RESULTS:**
149
150 **Residues 44-53 in the ExbD disordered domain are essential for TonB system activity.**
151 In our previous study, deletions that encompassed most of the disordered domain of ExbD
152 protein, (Δ42-51) and (Δ52-61), were completely inactive because they eliminated the ability of
153 its partner protein, TonB, to undergo essential conformational changes in response to change
154 in PMF (35). The effects of these deletions could have been due to structural distortions. To
155 circumvent that issue, here we engineered and characterized ExbD mutagenized with blocks
156 of Alanine substitutions to identify functionally important residues within the disordered domain
157 (Fig. 1B): ExbD (44-48Ala), ExbD (49-53Ala), ExbD (54-58Ala), and ExbD (59-63Ala). TonB
158 system activity was determined by measuring the initial transport rates of two different iron-
159 siderophores, $^{55}$Fe-enterochelin and $^{55}$Fe-ferrichrome to identify any TonB-dependent
160 transporter-specific activities (7, 40).

161 Both ExbD (54-58Ala) and ExbD (59-63Ala) transported $^{55}$Fe-enterochelin or $^{55}$Fe-
162 ferrichrome at rates equivalent to the wild-type ExbD encoded on pKP999 (pExbD), identifying
163 them as being in the mutation-tolerant half of the disordered domain. In the mutation-intolerant
164 half, neither ExbD (44-48Ala) nor ExbD (49-53Ala) were able to transport either siderophore.

165 ExbD (59-63Ala) required significantly more sodium propionate (20 mM) to achieve
166 chromosomal ExbD levels, suggesting that it was important for proteolytic stability (Fig. 2).
167 These results excluded residues 54-63 as functionally important for the TonB system and
168 eliminated the possibility of siderophore-specific effects.

169 Previously, ExbD (Δ42-51) and ExbD (Δ52-61) were unable to form the formaldehyde-
170 cross-linked ExbD-TonB complex that typifies Stage III (35). Consistent with that, the inactive
171 ExbD (44-48Ala) and ExbD (49-53Ala) had the same cross-linking profile in the presence and
172 absence of TonB, indicating that they could not form that Stage III complex. In contrast, for the
173 active ExbD (54-58Ala), and ExbD (59-63Ala), the absence of TonB led to the absence of the
174 formaldehyde cross-linked ExbD-TonB complex (Fig. S1).

175 To test whether the absence of the PMF-dependent ExbD-TonB complex was due to
176 the ability of ExbD (44-48Ala) and ExbD (49-53Ala) to somehow induce proton leakage, we
177 measured the rate of PMF-dependent ethidium bromide efflux through the AcrA/AcrB/TolC
178 complex (41, 42). None of the block Ala mutants came close to PMF leakage caused by 15 μM
179 CCCP, which nonetheless still supports 100% $^{55}$Fe-ferrichrome transport (data not shown)
180 (Fig. S2A). Because PMF was adequate for $^{55}$Fe-ferrichrome transport, the reason for the
181 inactivity of the block Ala substitutions must lie elsewhere.

182 Expression of ExbD (44-48Ala) did, however, cause a small but statistically significant
183 increase in ethidium bromide accumulation compared to pExbD (Fig. S2B). The means by
184 which ExbD (44-48Ala) caused this low level of proton leakage was unclear, especially since
185 the Δ*exbD* strain with *tolQR* present did not detectably leak protons (data not shown). Because
186 there is crosstalk between the TonB system and the Tol-Pal system (43), and because
187 RA1045 (Δ*exbD*, Δ*tolQR*) showed the same degree of proton leakage as ExbD (44-48Ala), we

188 speculate that proton leakage could have been induced by TolA in the absence of TolQR or a
189 functional ExbBD.

190

191 ***In vivo* photo-cross-linking identifies characteristic PMF-dependent and novel PMF-**
192 ***in*dependent ExbD-TonB complexes.** Disordered domains of proteins are often regions of
193 interaction with other proteins (44). ExbD and TonB, both of which contain regions of disorder,
194 form a formaldehyde cross-link, but the residues involved are unknown (29). To identify
195 contacts made by the ExbD disordered domain, individual amber mutations were constructed
196 at codons 44-63. The photoreactive, non-natural amino acid, *p*-benzoyl-L-phenylalanine
197 (*p*Bpa) was incorporated at the site of each amber mutation and used to covalently capture
198 protein interactions within 3 angstroms upon exposure to ultraviolet (UV) light (45, 46). The
199 advantage of this approach over formaldehyde cross-linking is that interactions through
200 defined sites can be investigated, while leaving the positions of residues in binding partners
201 unconstrained.

202 To characterize ExbD-TonB interactions made through the ExbD disordered domain, we
203 chose ExbD (S54pBpa) and ExbD (R59pBpa) as representatives for photo-cross-linking. Both
204 variants were active in iron transport assays and shared representative complexes with the
205 rest of the pBpa substitution mutants (shown below). On immunoblots developed with anti-
206 TonB monoclonal antibodies, two different ExbD-TonB complexes were captured by both
207 variants, a doublet at ~55 kDa and a single band at ~46 kDa (Fig. 2, lanes 4 and 8). Because a
208 C-terminally added $His_6$ epitope tag on ExbD caused each of the complexes to migrate at a
209 higher apparent mass equivalent to that of the added $His_6$ tag, all the bands consisted of TonB
210 complexed with full-length ExbD (Fig. 2, lanes 11 and 12). No complexes were detected in a
211 strain where the *tonB* gene was deleted (Fig. 2, lane 7).

212 The sole potentially proton-responsive amino acid in the TonB system, Asp 25, resides
213 in the TMD of ExbD [Fig.1; (15, 36)]. ExbD (D25N) is a well-characterized inactive mutant
214 which causes the TonB energization cycle to stall at Stage II and is therefore useful for
215 differentiating between PMF- dependent and -*in*dependent ExbD interactions (29, 35, 47).
216 Complexes decreased or eliminated by ExbD (S54pBpa) or ExbD (R59pBpa) in concert with
217 the D25N mutation identified the ~55 kDa doublet as being PMF-dependent (Fig. 2, lanes 5
218 and 9). Consistent with that observation, the same complexes were also eliminated by
219 treatment with the protonophore cyanide *m*-chlorophenylhydrazone (CCCP) (Fig. 2, lanes 6
220 and 10). Although the reason for the doublet was not clear, it appeared to represent two
221 different PMF-dependent sites of contact made by ExbD (S54pBpa) and ExbD (R59pBpa) with
222 TonB.

223 In contrast, the abundance of ~46 kDa ExbD-TonB complex was undiminished by the
224 presence of the ExbD D25N mutation or by CCCP treatment, indicating that it formed
225 independently of whether or not PMF was present. The ExbD D25N variant generated
226 somewhat higher levels of the ~46 kDa complex, consistent with the idea that it stalls TonB at
227 Stage II, where such complexes build up (34). These data demonstrated that loss of PMF
228 caused a significant change in the sites through which ExbD disordered domain residues
229 contact TonB—enough difference that it resulted in a change in the apparent mass of
230 complexes from ~55 kDa to ~46 kDa.

231 We knew that ExbD and TonB made *in vivo* contacts through their extreme C-termini
232 (38, 39). We did not know that additional ExbD contacts occurred so close to the ExbD (and,
233 presumably, TonB) TMDs (Fig. 1A,B).

234

235 **Most of the pBpa substitutions in the ExbD disordered domain capture some form of**
236 **TonB contact.** To understand the full extent of interactions between the ExbD disordered
237 domain and TonB, *in vivo* photo-cross-linking was carried out through pBpa substitutions at
238 ExbD codons 44-63. Most pBpa substitutions in the region from 44-52 supported significantly
239 reduced TonB-dependent $^{55}$Fe transport activity (< 25% wild-type levels), consistent with the
240 results from the block Ala substitutions which essentially eliminated activity (compare Figs.2
241 and 4A). Substitutions at residues 53-63 all supported at least 50% activity except for ExbD
242 (R59pBpa) which also supported only 25% activity. Several single pBpa substitution mutants
243 from residues 54-63 were less active than ExbD (54-58Ala) and ExbD (59-63Ala) (compare
244 Fig. 2A with Fig. 4A, right panel). The bulky pBpa side chain was likely responsible for the
245 discrepancy, possibly alluding to the importance of conformational flexibility or lock and key fit
246 for these residues. Nonetheless, except for ExbD (V45pBpa) and ExbD (V47pBpa), all the
247 pBpa substitutions within the ExbD disordered domain had detectable levels of activity.
248 Therefore, the complexes captured by these substitutions at least identified TonB proteins
249 within ~3angstroms of the pBpa moiety (46), and likely reflected functional interactions that
250 occurred during a TonB energization cycle.

251 The PMF-dependent ExbD-TonB complexes formed starting at approximately ExbD
252 residue A51(pBpa) and continuing through P63 (pBpa), with all the pBpa substitutions except
253 S52(pBpa) participating (Fig. 4B). Consistent with the intrinsically disordered nature of this
254 region and the already known changes in protein-protein interactions that must occur during an
255 energy transduction cycle, there was not a strong pattern of interaction suggestive of an $\alpha$-
256 helix or $\beta$-sheet (24, 35, 37).

257 We had previously observed a PMF-dependent formaldehyde-cross-linked ExbD-TonB
258 complex, but did not know through which residues of the ExbD periplasmic domain it occurred

259 (29). The ExbD disordered domain contains only three formaldehyde-cross-linkable residues:
260 K46, R59, and K62 (48). ExbD (K46pBpa) did not capture the PMF-dependent ExbD-TonB
261 interaction via photo-cross-linking, indicating that the PMF-dependent formaldehyde cross-
262 linked complex did not form through that residue (Fig. 4B, left panel). Similarly, because ExbD
263 (59-63Ala), which eliminated formaldehyde-crosslinkable residues R59 and K62, still captured
264 the PMF-dependent formaldehyde-cross-linked ExbD-TonB complex (Fig. S1), the idea that
265 the ExbD disordered domain participated in the previously observed PMF-dependent
266 formaldehyde cross-link to TonB could be ruled out.

267 The PMF-*in*dependent ExbD-TonB interaction characterized in Fig. 3, was captured by
268 the majority of the residues within the ExbD disordered domain (Fig. 4B). Because the
269 abundance of complex was fainter at either end of the range of pBpa substitutions, it could be
270 that the ExbD disordered domain constituted the PMF-*in*dependent interface. Interestingly, the
271 ExbD disordered residues that trapped the PMF-*in*dependent interactions were similar to an
272 ExbD interface predicted to interact with TonB by phage-panning experiments (49).

273 In addition to the ExbD-TonB PMF-dependent complex and ExbD-TonB PMF-
274 *in*dependent complex, there was also an unknown ~62 kDa complex trapped via photo-cross-
275 linking by ExbD (T53pBpa) and ExbD (Q57pBpa) (Fig. 4B). We do not know the identity of the
276 complex except that it certainly contains both ExbD and TonB.

277

278 **The ExbD disordered domain interacts with another ExbD and with ExbB.** ExbD also
279 formaldehyde cross-links *in vivo* into a single homodimeric complex (~ 30 kDa) and a single
280 heterodimeric complex with ExbB (~41 kDa) through unknown residues (29, 34). To determine
281 if the ExbD disordered domain formed similar complexes, we used ExbD (D44pBpa) and
282 (S54pBpa) as examples (Fig. 5A, B). In Fig. 5A, ExbD (D44 pBpa) formed complexes with

283 apparent masses of ~39 kDa and ~43 kDa, making them both, based on their apparent
284 masses, candidates to be potential ExbD-ExbB complexes. Surprisingly, the addition of a C-
285 terminal $His_6$ epitope tag to ExbB caused both complexes to shift to a higher mass consistent
286 with the added $His_6$ tag, indicating that both were ExbD-ExbB complexes. The presence of two
287 different ExbD-ExbB complexes indicated that either or both proteins were undergoing
288 conformational changes that influenced the nature of the contacts between them during the
289 energy transduction cycle.

290 In Fig. 5B, ExbD (S54pBpa) formed an ~31 kDa complex, consistent with an ExbD
291 homodimer. Addition of a C-terminal $His_6$ tag caused a decrease in the migration of the ~31
292 kDa complex consistent with the presence of two $His_6$ epitope tags, confirming that
293 identification. (Fig. 5B). ExbD (S54pBpa) also formed the ~ 46 kDa ExbD-ExbB complex and,
294 as expected, the ExbD-TonB PMF-dependent and -*in*dependent complexes.

295

296 **The majority of pBpa substitutions in the ExbD disordered domain capture contacts**
297 **with ExbB as well as ExbD.** To understand the full extent of interaction between the ExbD
298 disordered domain and itself or ExbB, we analyzed in vivo photo-cross-linking by the series of
299 ExbD (pBpa) substitutions by immunoblot with anti-ExbD antibody. As expected, the ExbD-
300 TonB PMF-dependent and -*in*dependent complexes could be discerned, but they were less
301 confidently identified due to the presence of other complexes in the same region of the
302 immunoblot, indicating that ExbD interacted with additional proteins, as seen in Fig. 5.

303 The ExbB-ExbD (upper, ~43 kDa) complex was prominently formed by residues from
304 the beginning of the ExbD disordered domain D44pBpa through P50pBpa, contacts that
305 placed the region adjacent to the predicted ExbD TMD, close to the small periplasmic regions
306 of ExbB, which mainly occupies the cytoplasm (Fig.1). Based on results with anti-TonB

307 antibodies (Fig. 4 lanes 5-10), it is likely that ExbD pBpa 46-50 lanes (Fig. 6, lanes 5-10) also
308 contain ExbD-TonB PMF-*in*dependent complex, which runs similarly to the ExbB-ExbD (upper,
309 ~43 kDa) complex and is therefore difficult to separately identify.-

310 The ~ 39 kDa ExbD-ExbB (lower) complex was formed by pBpa substitutions
311 throughout the disordered domain from D44 through P63 at similar intensities. This indicates
312 that a site in ExbD ~20 residues from its predicted periplasmic TMD boundary [residues 32-43,
313 (17)] binds to ExbB. The fact that ExbB has only a 20-residue periplasmic loop and a 21-
314 residue periplasmic amino terminus raises the possibility that the ExbD disordered domain was
315 condensed at some point during the TonB energization cycle such that it was closer to the
316 inner-membrane (15). Alternatively, the ExbB periplasmic N-terminus might extend into the
317 periplasm.

318 In contrast to the ExbD-TonB complexes, the ExbD-ExbD homodimers were captured
319 more efficiently in the mutation-intolerant half of the ExbD disordered domain, residues 44-49
320 and 52-55, without emergence of a pattern indicative of structural elements.

321

322 **The ExbD disordered domain contains a conserved ΨXΨXLP motif.** A multiple sequence
323 alignment of the ExbD disordered domain was generated and displayed in a sequence logo
324 using HHblits in the Gremelin.bakerlab program of all sequences within an expect score of $e^{-10}$
325 of *Escherichia coli K-12 strain* (NP_417478.1) (Fig. 7A). The sequence logo identified a
326 ΨXΨXLP motif where the psi symbol (Ψ) represents large aliphatic side-chained residues and
327 X represents any non-hydrophobic residue (Fig. 7B). The motif consisted of residues V45,
328 V47, L49, and P50, which reside in the mutation-intolerant segment of the disordered domain
329 and were also conserved in the *Escherichia coli* ExbD paralog, TolR of the Tol system, but not
330 in paralog MotB of the flagellar motor (Fig. 7B). There is modest crosstalk between the TonB

331 and Tol systems such that they can substitute functionally for one another. However, to our
332 knowledge, MotAB does not participate in any crosstalk. Cross-talk has been assumed to be
333 due to the similarities between ExbB/ExbD TMDs of the TonB system and TolQ/TolR TMDs of
334 the Tol system (21, 43, 50). Conservation of the ΨXΨXLP motif in both TolR and ExbD
335 suggested that an additional source of cross-talk between ExbB/ExbD and TolQ/R might exist.

336

337 **Only ExbD motif residues V45, V47, L49 and P50 are important for TonB system activity.**

338 Assessment of the activities of the pBpa substitutions in the mutation-intolerant segment
339 showed that the least active ones [V45(pBpa) and V47(pBpa)], were part of the ΨXΨXLP motif
340 (Fig. 4A). To better define the motif, individual Alanine substitutions were constructed in ExbD
341 from residues 44 through 53. ExbD variants carrying V45A, V47A. L49A, and P50A mutations
342 were the only ones with deficits in initial $^{55}$Fe-ferrichrome transport rates significantly below
343 90% of pExbD, with activities of 32%, 21%, 34%, and 50%, respectively (Fig. S3). Thus V45,
344 V47, L49 and P50 were the only functionally important residues within the entire ExbD
345 disordered domain.

346 To further define the motif, each of the V45A, V47A, L49A, and P50A substitutions in
347 the motif region was combined with the others to create six double Ala substitutions. Had these
348 mutations been simply additive in their effects, we would have seen that, for example, the
349 V45A, P50A double mutant should have ~16% activity (50% of 32%). Instead, this double
350 mutant, like all six double mutants, was inactive in $^{55}$Fe-ferrichrome transport, suggesting a
351 degree of synergy between them (Fig. 8A). However, the iron transport assays do not
352 discriminate well among low levels of TonB system activity (51).

353 Colicins toxins are synthesized by some *E. coli* to kill sensitive strains. B-group colicins
354 use the TonB system and its corresponding TBDTs to cross the outer membrane of *E. coli* to
355 gain access to their targets in the periplasm, cytoplasmic membrane or cytoplasm (52). Colicin
356 sensitivity assays, while not as discriminative among higher levels of TonB system activity, can
357 detect the activity supported by as little as one molecule of TonB (51). To determine whether
358 the double Ala substitutions could support any activity, their sensitivity to B-group colicins B, Ia,
359 and M was tested (Fig. 8B). All of the double-Ala mutants were tolerant (insensitive) to virtually
360 all colicins tested, suggesting that the motif residues do not work independently of each other
361 and validating the identification of this motif.

362

363 **ExbD (V45A, V47A) and ExbD (V47A, L49A) stall TonB at Stage II of the energy**
364 **transduction cycle.** ExbD regulates TonB conformational changes as TonB moves through
365 an energy transduction cycle (6, 34). Stage II of the TonB energization cycle is a PMF-
366 *in*dependent Stage where the N-terminal ~ 155 residues of TonB (an ~23 kDa fragment) are
367 protected from proteinase K degradation if full-length ExbD is present, although an actual
368 complex between the two proteins had not been observed until this study (Fig. 5). Heretofore,
369 Stage II had been detectable only when PMF was collapsed, preventing TonB from moving on
370 to Stage III. When PMF, ExbB, ExbD, and TonB are all present and active, TonB automatically
371 transitions from Stage II to Stage III, rendering TonB fully sensitive to proteinase K. Our
372 observation that ExbD (44-48Ala) and ExbD (49-53Ala) failed to form a Stage III formaldehyde
373 cross-link suggested that the effects of substitutions in the disordered domain motif might be to
374 stall TonB at Stage II (Fig. S1). Since only ExbD residues V45, V47, L49, and P50 were
375 important for ExbD activity, we assessed whether the inactive double mutants (V45A, V47A),
376 (V47A, L49A) and (L49A, P50A) were required for TonB to proceed beyond Stage II based on

377 its sensitivity to exogenously added proteinase K in spheroplasts. For comparison, we
378 assessed the proteinase K accessibility of ExbD (D25N).

379 The hallmarks of the ExbD (D25N) mutant, where TonB is permanently stalled at Stage
380 II are 1) that TonB forms a proteinase K-resistant fragment in both the presence and absence
381 of CCCP and 2) that TonB is unable to remain in its stalled Stage II proteinase K-resistant
382 conformation over time [Fig. 9, panel 4 +/- CCCP; (34)]. As expected, the Δ*exbD,* Δ*tolQR*
383 strain did not support the ability of TonB to form the ~23 kDa proteinase K-resistant TonB
384 fragment [Fig. 9, panel 3]. A ~28 kDa TonB fragment, seen previously and typified by Δ*exbD,*
385 Δ*tolQR* and ExbD (D25N) in panels 3 and 4, does not appear to have relevance to the
386 mechanism of TonB energization (34).

387 ExbD (V45A, V47A) and ExbD (V47A, L49A) largely mimicked the effect of ExbD
388 (D25N) on TonB, leaving it stalled in Stage II (Fig. 9). Together the results suggest that the
389 ExbD ΨXΨXLP motif was required for TonB to transition from Stage II to Stage III of the
390 energization cycle. ExbD (L49A, P50A) was too sensitive to proteinase K to be evaluated (Fig.
391 9 panel 7).

392

393 **The ExbD disordered domain ΨXΨXLP motif is required for correct configuration of the**
394 **ExbD C-terminus.** To better understand why the ExbD ΨXΨXLP motif left TonB stalled in
395 Stage II, we combined the V45A, V47A double mutation with pBpa substitutions along the
396 length of ExbD: E14(pBpa)— presumably cytoplasmically localized based on the topology of
397 ExbD; I24(pBpa)—in the ExbD TMD; S54(pBpa)—in the mutation-tolerant segment of the
398 disordered domain; S67(pBpa)—just beyond the disordered domain; K97(pBpa)—a known
399 point of ExbD-TonB contact through engineered Cys residues (39); and E136(pBpa)—near the
400 C-terminus. With the exception of ExbD (I24pBpa), the other substitutions were active.

401 Plasmid-encoded ExbD E14pBpa, S67pBpa, K97pBpa, and E136pBpa substitutions were
402 72%, 24%, 90%, and 100% of $^{55}$Fe-Ferrichrome transport of pKP999 + pEVOL in RA1045.

403 Overall, the double V45A, V47A substitutions did not have much effect on ExbD photo-
404 cross-links to TonB through distal pBpa substitutions, except for (S54pBpa) where it greatly
405 diminished the PMF-dependent ExbD-TonB complex (Fig. 10A lanes 6,7). ExbD (E14pBpa), in
406 the cytoplasm, did not form complexes with TonB (Fig. 10A, lanes 4,5), however, ExbD
407 (I24pBpa), in the TMD, formed a PMF-*in*dependent TonB complex (Fig. 10A lanes 6,7),
408 indicating that at some point in its energy transduction cycle, TonB was in close proximity to
409 ExbD through their TMDs. ExbD (K97pBpa) and ExbD (E136pBpa) also formed PMF-
410 *in*dependent Stage II complexes with TonB (Fig. 10A, lanes 6,7,12-15). We do not know why
411 the level of monomer was consistently reduced for ExbD (K97pBpa), but it clearly did not
412 prevent capture of ExbD-TonB complexes.

413 Among the periplasmic pBpa substitutions tested, the presence of the V45A, V47A
414 double substitution caused ExbD to photo-cross-link to a variety of unknown proteins,
415 especially ExbD V45A, V47A (S54pBpa), which captured approximately eight different
416 complexes with unknown proteins (Fig. 10B, lane 9). Furthermore, ExbD (E136pBpa) V45A,
417 V47A captured two prominent complexes with unknown proteins (Fig. 10B, lane 15). These
418 results showed that the conserved motif within the disordered domain of ExbD was important
419 for correctly regulating contacts made by the ExbD C-terminus.

420

421 **DISCUSSION:**

422 TonB-dependent energy transduction is cyclic, with TonB, anchored in the inner
423 membrane, engaging and disengaging from a TBDT as it energizes active transport across the
424 outer membrane. Understanding the molecular interactions among TonB system proteins in

425 the cytoplasmic membrane--ExbB, ExbD, TonB--and the TBDTs in the outer membrane is
426 essential to understanding the mechanism of this novel dual-membrane transport system.

427 Our current model consists of multiple Stages that occur prior to productive TonB
428 energy transmission to a TBDT [Fig. 11; (24, 34)]. In Stage I, TonB and ExbD homodimers are
429 each found in separate complexes with ExbB homotetramers which do not interact. In Stage II,
430 the ExbB-TonB and ExbB-ExbD oligomeric complexes come together to form a multimeric
431 heterocomplex consisting of all three proteins, in which the first ~155 residues of TonB are
432 protected from digestion by exogenous addition of proteinase K to spheroplasts. Prior to our
433 work here, Stage II could only be detected when the PMF was artificially collapsed by addition
434 of the protonophore CCCP. We also knew that ExbD was somehow required to form the
435 proteinase K-resistant fragment of TonB. However, prior to this study, we had not been able to
436 detect the TonB-ExbD PMF-*in*dependent complex in Stage II, although its existence was
437 implied. Nor had we been able to determine precisely through which residues the PMF-
438 *in*dependent Stage II complex formed. From Stage II the TonB system transitions to Stage III,
439 characterized by a requirement for PMF and a formaldehyde-cross-linked complex containing
440 both ExbD and TonB. The final Stage in our current model is Stage IV in which TonB that has
441 been properly reconfigured by ExbD binds the TBDT in such a manner that active transport
442 across the OM occurs (6). After Stage IV, the multimeric heterocomplex of ExbB, ExbD, and
443 TonB breaks down into isolated complexes of ExbB-ExbD, ExbB-TonB, and a minor fraction of
444 free-floating ExbB (24)

445

446 **The ExbD disordered domain is highly dynamic.** *In vivo* photo-cross-linking has the
447 advantage of potentially capturing every interaction within ~3 angstroms that a single pBpa
448 substitution is involved in during the TonB energization cycle (46). Throughout the ExbD

449 disordered domain (residues 44-63 immediately distal to its TMD), each single ExbD residue
450 captured multiple complexes. Disordered domains of proteins are known to have a high degree
451 of conformational plasticity that can mediate changes in protein oligomerization and function
452 (53). For example, substrate binding to the intrinsically disordered domain of periplasmic
453 protease/chaperone DegP causes a change from proteolytically inactive hexamers to
454 proteolytically active polyhedrons consisting of 4, 6, and,8 trimers (54, 55).

455 Consistent with characteristics of disordered domains, most of the ExbD pBpa
456 substitutions within the disordered domain captured at least four out of five identifiable
457 complexes (ExbD homodimer, two ExbD-ExbB complexes, and two ExbD-TonB complexes)
458 through a single pBpa substitution. This indicated that residues within the ExbD disordered
459 domain underwent multiple partner swaps during the Stages of the TonB energization cycle
460 and quantified the minimum number of disordered domain contacts that occurred.

461 ***ExbD-TonB complexes*** – TonB is predicted to have large regions of intrinsic disorder
462 starting immediately after its TMD, suggestive of multiple sites through which protein-protein
463 interactions occur (56). Consistent with that, the dimeric crystal structures of the TonB C-
464 terminus do not exist in vivo, even though TonB homodimerizes through that domain in vivo
465 (26). Because TonB contains no single essential residue (26, 36, 56-60), ExbD is
466 hypothesized to determine the final configuration of TonB that is capable of transducing energy
467 to TBDTs (21, 26, 29, 34). As pBpa substitutions, different subsets of residues within the ExbD
468 disordered domain (residues 44-63) captured both PMF-*in*dependent and PMF-dependent
469 ExbD-TonB interactions using *in vivo* photo-cross-linking. For the first time, a PMF-
470 *in*dependent ExbD-TonB complex was captured, which validated the previously predicted
471 existence of Stage II in the TonB energization cycle.

472 A PMF-*in*dependent Stage II complex was formed by residues from 44-63--nearly all the
473 disordered domain. The size of the ExbD disordered domain that captured this interaction was
474 much smaller than the ~ 155 residues of TonB protected against proteinase K degradation by
475 ExbD (6). Either the full length of ExbD (~ 141 residues) can directly protect TonB or, as has
476 been proposed previously, the disordered domain of ExbD induces conformational changes
477 that render the TonB protease-insensitive (21, 60). Previous disulfide cross-linking
478 experiments with engineered Cys substitutions within ExbD residues 92-121 failed to capture a
479 PMF-*in*dependent interaction (38, 39).

480 PMF-dependent ExbD-TonB complexes were captured only by the more distal end of
481 the disordered region through ExbD residues A51, and T53 to P63. We previously showed that
482 deletions of residues 42-51 and 52-61 prevented formation of the PMF-dependent Stage III
483 ExbD-TonB complex, but did not know if those regions were directly or indirectly responsible
484 (35). We showed here that the ExbD disordered domain directly contacted TonB PMF-
485 dependently. Thus, we identified another ExbD region besides residues 92-121 that requires
486 PMF for interaction with TonB. However, like the ExbD region of 92-121 Cys substitutions, Ala
487 substitutions for the ExbD disordered domain residues that captured the PMF-dependent
488 ExbD-TonB interaction did not significantly decrease TonB system activity. This may suggest
489 that the disordered domain and the 92-121 residue region are simply the read-outs for PMF-
490 dependent events initiated elsewhere in ExbD, possibly through its TMD, which contains the
491 only potentially PMF-responsive residue in the TonB system (15, 29, 36). It also cannot be
492 ruled out that some functionally important ExbD disordered residues (i.e. V45 and V47) directly
493 interact with TonB PMF-dependently, but due to their low activity, the interaction was not
494 captured.

495 ***ExbD-ExbB complexes*** - ExbD and ExbB formaldehyde cross-link into a complex of
496 complex of ~41 kDa (29).Surprisingly, two distinct ExbD-ExbB complexes were captured via
497 photo-cross-linking: an ~ 39 kDa (lower) complex and an ~43 kDa (upper) complex. While both
498 techniques are probes for close contacts, formaldehyde cross-linking occurs through residues
499 W, H,Y,R,C, K and N-termini and requires that both proteins have these specific residues in
500 close proximity for the cross-link to occur (48). Photo-cross-linking, on the other hand, allows
501 crosslinking to occur between the engineered site containing pBpa and any carbon-hydrogen
502 bonds within ~ 3 angstroms (46). In addition, the apparent mass of a complex can vary with the
503 sites through which the two proteins are linked (61). The difference in the masses of
504 formaldehyde cross-linked and photo-cross-linked may therefore be due to differences in the
505 sites of complex formation. We can say, however, at a minimum, there are two different forms
506 ExbD-ExbB complexes that suggest a single pBpa residue binds to two different regions of
507 ExbB as the energy transduction cycle proceeds. If so then, it would suggest that in only one
508 of these interactions are the formaldehyde-cross-linkable residues in correct apposition in both
509 ExbD and ExbB.

510 The ~ 39 kDa ExbB-ExbD (lower) complex was captured with similar intensities by all
511 residues in the ExbD disordered domain. ExbB has few of its residues in the periplasm: an ~
512 21-residues N-terminus and ~ 26-residue loop between TMDs 2 and 3 (14, 15). The
513 topological relationship between the ExbD disordered domain and ExbB suggest that either
514 ExbB sequences assume extended conformations or that the ExbD disordered domain moves
515 close to the membrane at some point during the TonB energization cycle. The latter possibility
516 would be consistent with one of the three ExbB-ExbD structures isolated and mapped via 3D
517 electron microscopy with ratios 4:2 in which electron density of the ExbD periplasmic domain is
518 parallel with the membrane (62). It would also be consistent with a genetic suppressor of

519 mutants in the ExbB paralog TolQ that map to C-terminus of the ExbD paralog, TolR in the Tol
520 system (63).

521 The ~43 kDa ExbD-ExbB (upper) complex was captured essentially only through the six
522 residues immediately distal to ExbD TMD. Unlike the ~ 39 kDa ExbD-ExbB complex described
523 above, this one could be based solely on proximity of the reactive ExbD pBpa residue to
524 periplasmic ExbB residues that were equally adjacent to the cytoplasmic membrane. Taken
525 together, the difference in apparent masses and different interaction profiles of the ~ 39 and ~
526 43 kDa complexes indicated that ExbD was in two different conformations in each complex
527 and likely interacting with different parts of ExbB.

528 When the TonB C-terminus is intact, its extreme N-terminus (L3C) is protected from
529 labeling by the thiol-specific membrane-permeant reagent Oregon Green® 488 maleimide;
530 when the TonB C-terminus is absent, TonB L3C is labeled (58). This behavior suggests two
531 different conformations of ExbB cytoplasmic domains, one which protects the TonB L3C from
532 labeling during binding of TonB to a TBDT and one which allows TonB L3C labeling when the
533 TonB C-terminus is engaged with ExbD (28). Perhaps, the two photo-cross-linked ExbD-ExbB
534 complexes in this work are related to ExbB conformational changes that influence the Oregon
535 Green® 488 maleimide labeling of cytoplasmic tail mutant TonB (L3C) as TonB moves through
536 an energy transduction cycle. Addition of CCCP did not prevent formation of the ExbB-ExbD
537 (upper) or ExbB-ExbD (lower) photo-cross-linked complexes, ruling out the possibility that
538 either was dependent on PMF.

539 ***ExbD-ExbD complexes*** - An ExbD homodimer (~31 kDa) identified using *in vivo* photo-
540 cross-linking had a similar apparent mass as the formaldehyde-cross-linked ExbD homodimer
541 (~30 kDa) (29). Except for ExbD (P50pBpa) and ExbD (A51pBpa), the intensity of the ExbD
542 homodimer complex gradually decreased as residues grew more distant from the TMD.

543 Because the residues that capture ExbD homodimers are immediately distal to its TMD, it
544 suggested that the ExbD TMDs were also homodimerized.

545

546 **The *in vivo* data compared to recent ExbB/ExbD structures** The ratio of cytoplasmic
547 membrane proteins ExbB, ExbD and TonB in vivo is 7ExbB:2ExbD:1TonB under four different
548 conditions of iron availability (13). This oddly asymmetric ratio played an important role in our
549 model of the TonB system (24, 30). In vitro, the ratios of these proteins in purified structures
550 are varied with none of them actually accounting for the cellular ratio, and with TonB protein
551 included in only one: 4ExbB: 2ExbD and 4ExbB: 1ExbD: 1TonB from single particle EM
552 studies (49, 62); 5ExbB:1ExbD and 6ExbB:3ExbD from crystal structure determinations (64,
553 65); 6ExbB:1ExbD from mass spectrometry (66); and most recently, 5ExbB: 2ExbD from cryo-
554 EM (67).

555 Recently, two crystal structures and a cryo-EM structure provide the first detailed view
556 of ExbB monomers, arranged front to back and forming a pore: 5 ExbB with 1 ExbD TMD in
557 the pore (crystal); 6 ExbB: 3 ExbD TMD in the pore (crystal); 5 ExbB: 2 ExbD TMD in the pore
558 (cryo-EM) (64, 65, 67). The ExbB monomers are a major and very important accomplishment
559 and are consistent with the known topology of ExbB; the oligomeric structures diverge from
560 what is known *in vivo* about ExbB oligomers, ExbD and TonB:

561 1) In vivo, ExbB formaldehyde-crosslinks into tetramers that are dimers of
562 homodimers. ExbB can also form disulfide-linked homodimers through D211C (30).
563 The D211 residues are not sufficiently close in the front-to-back configuration of ExbB
564 monomers in crystal and cryo-EM structures to form disulfide-linked homodimers (64,
565 65, 67).

566 2). In vivo, ExbB formaldehyde-cross-links to TonB and TonB interacts with
567 ExbB TMD1 (15, 29, 30, 68). None of the recent ExbB crystal or cryo-EM
568 pentameric/hexameric structures includes TonB (64, 65, 67).

569 3). In the recent ExbB crystal and cryo-EM structures, TonB is proposed to be
570 outside the pore formed by the ExbB pentamer/hexamers because the lumens of the
571 pores are entirely filled with one-to-three ExbD TMDs (64, 65, 67). Because TonB is
572 known to go through its energy transduction cycle homodimerized through or near its
573 TMD (24), the crystal and cryo-EM structures give rise to a ratio of 5-6 ExbB:10-12
574 TonB—the converse of the cellular ratio of 14 ExbB:2 TonB.

575 4) The *in vivo* photo-cross-linking data from this study indicated that ExbD
576 (I24pBpa) in the ExbD TMD, as well as most of the immediately adjacent periplasmic
577 ExbD disordered domain captured the ExbD-TonB PMF-*in*dependent complex. This
578 strongly suggested that ExbD and TonB TMDs interact in vivo. As noted in point 3
579 above, neither the recent crystal nor cryo-EM structures of ExbB oligomers permits
580 ExbD and TonB to interact through or near their transmembrane domains because the
581 lumens of the ExbB pores are fully occupied by ExbD TMDs (64, 65, 67).

582 The discrepancies between *in vivo* results and ExbB crystal and cryo-EM structures
583 raise questions about the validity of the structures and their possible roles in TonB-dependent
584 energy transduction. Our current model identifies Stages in that process (24), and in this study,
585 we identified dynamic contacts among ExbD, TonB and ExbB that occurred during those
586 Stages through identical pBpa substitutions, changing as TonB moved through an energy
587 transduction cycle. Perhaps the *in vitro* structures approximate a version of Stage I where the
588 ExbB tetramers bind ExbD homodimers or TonB homodimers, but not both together (24).

589

590 **The ExbD ΨXΨXLP motif is required for signal transduction** Single Ala substitutions in the
591 ExbD ΨXΨXLP motif (V45, V47, L49, P50) decreased but did not eliminate TonB system
592 activity. Evidence for its importance as a motif came from combining the Ala substitutions, all
593 of which double combinations were virtually inactive, even in the most sensitive assays
594 capable of detecting one active molecule of TonB (51).

595 In this study we discovered that the ExbD ΨXΨXLP motif (V45, V47, L49, P50) played a
596 role in signal transduction to both TonB and to its own C-terminal domain. First, we were able
597 to identify the step mediated by the ΨXΨXLP motif within the context of our current model for
598 TonB energization (Fig. 11). The double mutation (V45A, V47A) prevented formation of Stage
599 III PMF-dependent ExbD-TonB complexes mediated through S54pBpa and K97pBpa, stalling
600 the TonB energization cycle in Stage II, just after ExbD and TonB were brought together, but
601 before they were able to form the PMF-dependent complex. Consistent with that, the double
602 mutation (V45A, V47A) did not prevent formation of the PMF-*in*dependent ExbD- TonB
603 complex, which ruled out the motif out as the site of contact.

604 Second, the V45A,V47A double mutation also caused pBpa substitutions in all four C-
605 terminal ExbD residues tested (S54, S67, K97, and E136) to form complexes with unknown
606 proteins. This was most notable in the case of S54pBpa where approximately eight new
607 complexes with unknown proteins were captured. It appeared therefore that the ΨXΨXLP
608 motif was important for transducing conformational signals to the ExbD C-terminus, which,
609 when not properly directed, had a pluripotent capacity to interact widely.

610

611 **MATERIALS and METHODS:**

612 **Strains and plasmids.** Strains and plasmids used in these studies are listed in Table S1.
613 Strain KP1526 was constructed by P1*vir* transduction of Δ*exbD*::*cam* from RA1021 (W3110,
614 Δ*exbD*::*cam*) into KP1525 (W3110, Δ*tolQR*, *aroB*) [RA1021 was a kind gift from Ray Larsen
615 (35).] Plasmids encoding Alanine and amber substitution mutations in *exbD* were primarily
616 pKP999 derivatives. Amber substitutions in plasmids encoding ExbD (V45A, V47A) were
617 derived from pKP2171. To determine the identity of potential ExbB complexes, a $His_6$ epitope
618 tag was added to the C-terminus of ExbB in the plasmid pKP1657, which encodes the ExbBD
619 operon with and without the ExbD $D44_{am}$ mutation. Mutant plasmids were engineered using
620 extralong PCR. Primers are available upon request. All genes containing PCR-based changes
621 were verified by DNA sequencing at the Penn State Genomics Core Facility, University Park,
622 PA.

623 **Media and growth conditions.** Cultures were grown at 37˚C with aeration. Saturated cultures
624 in Luria-Bertani broth were sub-cultured in mid-exponential phase at 1:75 in M9 minimal media
625 supplemented with 0.4% glycerol, 0.2% Casamino Acids, 40 µg/ml tryptophan, 4 µg/ml vitamin
626 B1, 1 mM $MgSO_4$, 0.5 mM $CaCl_2$, and 37 µM $FeCl_3$. Plasmid-encoded ExbD and its variants
627 were expressed in RA1045 (W3110, Δ*exbD*, Δ*tolQR*) in the presence of 100 µg/mL ampicillin
628 unless otherwise noted. Sub-cultures in M9 medium were induced with sodium propionate
629 (ranging from 0-45 mM) to approximate the steady state levels of ExbD protein from W3110,
630 the wildtype control (Table S1). Subcultures were harvested by immediate precipitation with
631 ice-cold trichloroacetic acid (TCA) at an $A_{550}$ ranging from 0.40 to 0.60 (40).

632 ***In vivo* formaldehyde-cross-linking**. Equal numbers of bacteria were resuspended in sodium
633 phosphate buffer (pH 6.8) and treated for 15 min at room temperature with 1% formaldehyde
634 (Electron Microscopy Sciences Cat #15710) as previously described (29, 40). Following
635 formaldehyde treatment, bacteria were suspended in sample buffer, heated to 60° C, and

636 equal cell numbers were loaded in each well of 13% sodium dodecyl sulfate (SDS)-
637 polyacrylamide gels (69). ExbD complexes and TonB complexes were detected by
638 immunoblotting with ExbD-specific polyclonal antibodies and TonB-specific monoclonal
639 antibodies, respectively (13, 70). Equal loads were confirmed by Coomassie staining of the
640 PVDF membrane used for the immunoblot.

641 ***In vivo* photo-cross-linking.** Plasmid pEVOL encodes an orthogonal tRNA synthetase and a
642 corresponding orthogonal $tRNA_{CUA}$ that recognizes amber (UAG) codons (45). Plasmids with
643 amber substitutions in *exbD* were co-expressed with pEVOL in RA1045 (W3110, Δ*exbD*,
644 Δ*tolQR*) and processed as previously described (7). At $A_{550}$ of ~0.2, sub-cultures in M9 were
645 treated with 0.004**%** arabinose to induce expression of the tRNA synthetase/tRNA pair from
646 pEVOL, 0.8 mM the photo-cross-linkable amino acid p-Benzoyl-L-phenylalanine (pBpa;
647 Bachem AG, www.bachem.com) and levels of propionate required for ExbD protein expression
648 at near-chromosomal levels (Table S1). 2.0 $A_{550}$-ml were harvested at $A_{550}$ ~ 0.5, pelleted at
649 room temperature and resuspended in 2 mL supplemented M9 media (as described above
650 with 1.85 μM $FeCl_3$ instead of 37 μM, and without antibiotics, pBpa, and propionate). Equal
651 volumes of each sample were transferred into single wells of each of two 24-well plates (NEST
652 Cell Culture Plate, cat: 702001). One plate was irradiated with 365-nm light for 30 min on ice
653 and the second plate was incubated in the dark simultaneously for 30 min on ice. Samples
654 were precipitated with 10% TCA as described previously and processed for immunoblot
655 analysis with ExbD-specific polyclonal antibodies and TonB-specific monoclonal antibodies
656 (13, 70). Equal loads were confirmed by Coomassie staining of the PVDF membrane used for
657 the immunoblot.

658 **Initial rates of $^{55}$Fe-ferrichrome and $^{55}$Fe-enterochelin transport**. Cultures were grown as
659 described in media and growth conditions. Strains harboring plasmids with and without amber

660 substitutions in *exbD* were grown as described in the *in vivo* photo- cross-linking section. $^{55}$Fe-
661 ferrichrome assay and $^{55}$Fe-enterochelin assay were performed in triplicate as previously
662 described (40). To exclude competition from native enterochelin, $^{55}$Fe-enterochelin uptake was
663 assessed in *aroB* strains that were sub-cultured with additional phenylalanine (40 µg/ml) and
664 tyrosine (40 µg/ml) to compensate for their inability to synthesize aromatic amino acids (7). To
665 determine steady state levels of the different ExbD variants at the time of assay, samples were
666 precipitated with 10% TCA at the start of the assay and equivalent numbers of cells processed
667 for immunoblot analysis on 13% SDS-polyacrylamide gels. ExbD proteins were detected by
668 immunoblotting with ExbD-specific polyclonal antibodies (13, 70).

669 **Ethidium bromide accumulation.** Sub-cultures were grown in M9 medium as described
670 above. At $A_{550}$ of 0.5, 2 mL of cells were transferred to 4.5 mL disposable cuvettes (VWR Cat#
671 30620-276). Ethidium bromide (6.25 µM) was added to the cells, which were excited at 520
672 nm and fluorescence was detected using a Perkin-Elmer LS-55 fluorescence
673 spectrophotometer at 590 nm. The width of the excitation and emission slits was 15 nm.
674 Fluorescence emission data were collected every second for 3 minutes using the Time Drive
675 application from the FLWINLAB software. For CCCP controls, either 15 µM or 60 µM CCCP
676 was added two minutes prior to ethidium bromide. The ethidium bromide accumulation rate for
677 each sample was determined by linear regression and recorded as Fluorescence Units per
678 second (FU/sec) (42).

679 **Proteinase K Accessibility**. TonB sensitivity to proteinase K was performed as previously
680 described (35). Briefly, cultures were grown as described in M9 minimal media and converted
681 to spheroplasts. At 5 min prior to proteinase K treatment (25 µg/mL), samples were treated
682 with 60 µM CCCP dissolved in dimethylsulfoxide (DMSO), where indicated. Samples were
683 collected at 2 min, 5 min, 10 min, and 15 min following proteinase K treatment with the addition

684 of phenylmethylsulfonyl fluoride (1.0 mM) to inactivate proteinase K at the specified times.
685 Samples were precipitated with 10% TCA final concentration, suspended in sample buffer,
686 loaded with equal volumes on 13% SDS-polyacrylamide gels and detected via immunoblotting
687 with TonB-specific monoclonal antibodies (13, 70).

688 **Colicin Sensitivity Assay.** The colicin sensitivity assay was performed as previously
689 described (40). Strains expressing ExbD at chromosomal levels were grown to mid-
690 exponential phase in T-broth with 100 µg/ml ampicillin and with levels of propionate that
691 induced chromosomal levels of expression as confirmed by TCA precipitation of cultures and
692 comparison to W3110 on immunoblots. Strains were plated in T-top agar on T-plates
693 containing the same propionate concentrations and ampicillin as were used in the sub-
694 cultures. Five-fold dilutions of Colicins B, Ia, or M (Colicin B enters via FepA; Colicin Ia enters
695 via CirA; Colicin M enters FhuA) were spotted on the bacterial lawns and were incubated
696 overnight at 37°C. Scoring was reported as the highest dilution that produced clearing.
697 Sensitivity to each plasmid was assayed in triplicate.

698

699 **ACKNOWLEDGEMENTS:**

700

701 Support from NIAID for grant AI11322 to K.P. is gratefully acknowledged. We thank Erica
702 Johnson, Dakota Matson, and Molly Sweeney for engineering many of the mutant plasmids in
703 this study. We thank Anne Ollis for construction of strain KP1526.

# FIGURES:

**A.** **B.**

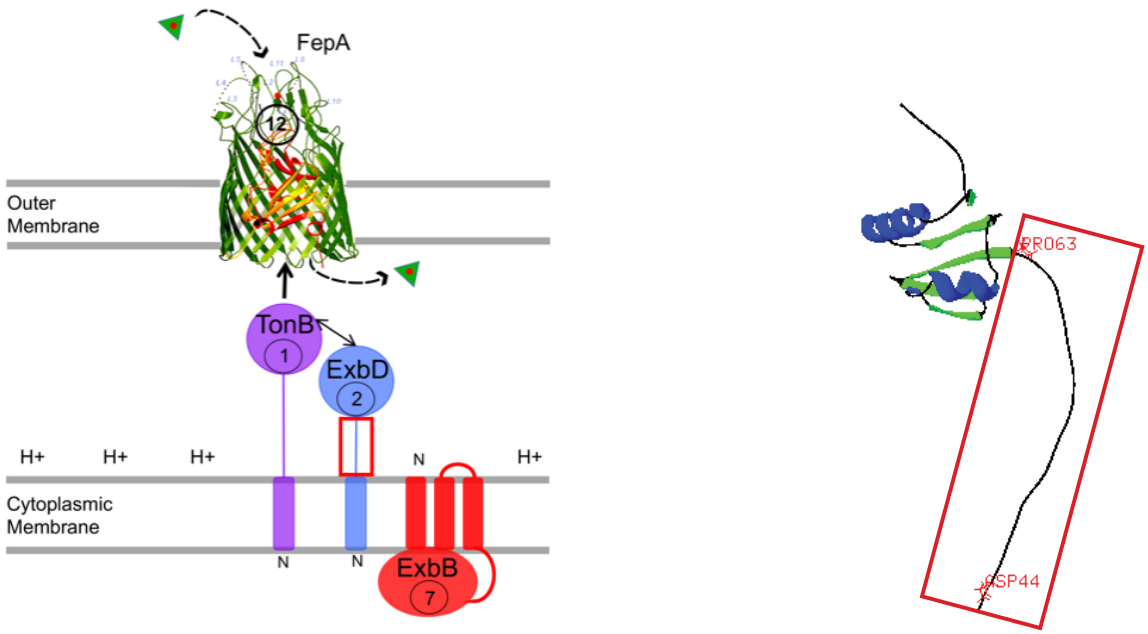


Figure 1: (A) TonB-dependent energy transduction. The iron-bearing siderophore enterochelin (triangles) binds to the TBDT FepA with sub-nanomolar affinity (71). This high affinity necessitates a mechanism to release the siderophore into the periplasmic space. In the presence of cytoplasmic membrane proteins TonB, ExbB, ExbD, and the cytoplasmic membrane proton motive force (PMF), the Fe-enterochelin is actively transported across the outer membrane through FepA. Numbers indicate the ratio of the proteins in *E. coli* under iron-limiting conditions (13). Because TonB is limiting, there must be a cycle during which TonB binds and releases TBDTs. The Stages in the cycle have been studied, resulting in a model where ExbB acts as a scaffold to manage an essential PMF-dependent interaction between TonB and ExbD that subsequently positions TonB for correct interaction with FepA. The red box around ExbD identifies the ExbD disordered region which is the topic of this study. Subsequent transport of enterochelin across the cytoplasmic membrane does not require the

721 TonB system [adapted from (24)]. (B) The NMR solution structure of ExbD periplasmic domain
722 residues 44-141 [NCBI PDB ID: 2PFU; (37)]. The alpha helices and beta strands are colored in
723 blue and green, respectively. The ExbD disordered region is boxed in red. The first residue
724 following the ExbD TMD, D44, and last residue, P63 of the ExbD disordered region are labeled
725 with the side chain displayed. This image was generated using Swiss-PdbViewer
726 [https://spdbv.vital-it.ch/(37)].

727

728

729

730

731

732

733

734

735

736

737

738

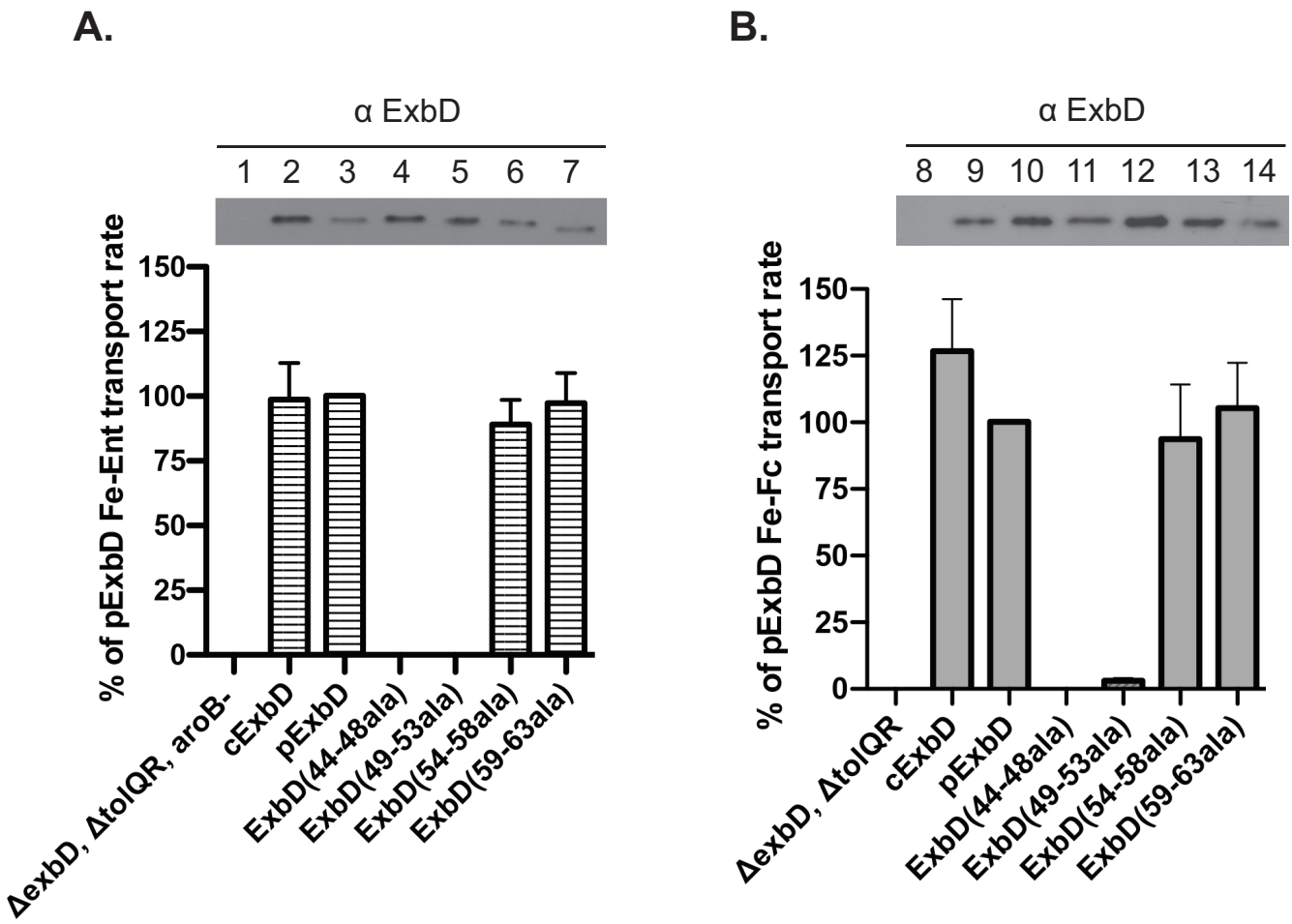


**Figure 2: Block Alanine substitutions of ExbD residues 44-48 and 49-53 prevent TonB system activity.** (A) Initial rate of $^{55}$Fe-enterochelin transport and corresponding steady-state expression levels of the ExbD proteins. Strains were grown to mid-exponential phase and assayed as described in Methods and Materials. The percentages of activity were calculated relative to the initial rate of plasmid-encoded ExbD, pExbD (pKP999), expressed at chromosomal levels in KP1526 (Δ*exbD*, Δ*tolQR, aroB*). Assays were performed in triplicate and carried out at least twice for each strain. The slopes were determined by a linear regression fit of scintillation counts per minute. The error bars indicate mean ± SEM for a representative triplicate set. The steady-state ExbD monomer levels at the time of assay were determined by immunoblot analysis (top). To avoid competition from enterochelin, the only siderophore synthesized by *Escherichia coli* K12 and transported by FepA (Fig. 1), *aroB*

751 strains were used. cExbD designates chromosomally expressed ExbD from the wild-type
752 strain, KP1270 (W3110, *aroB*). ExbD Alanine substitution mutants are expressed from
753 plasmids in KP1526 (Δ*exbD*, Δ*tolQR, aroB*). (B) Initial rate of $^{55}$Fe-ferrichrome transport and
754 corresponding steady-state expression levels of ExbD proteins. The assay was performed and
755 analyzed identically as in (A) using the siderophore, ferrichrome, which is transported through
756 the TonB-dependent transporter, FhuA. The percentages of activity were calculated relative to
757 the initial rate of plasmid-encoded ExbD, pExbD (pKP999) expressed at chromosomal levels in
758 RA1045 (Δ*exbD*, Δ*tolQR*). cExbD designates chromosomally expressed ExbD from the wild-
759 type strain, W3110. All ExbD Alanine substitution mutants are expressed from plasmids in
760 RA1045 (Δ*exbD*, Δ*tolQR*). The plasmid identities and concentrations of propionate for
761 chromosomal expression are listed in Table S1.

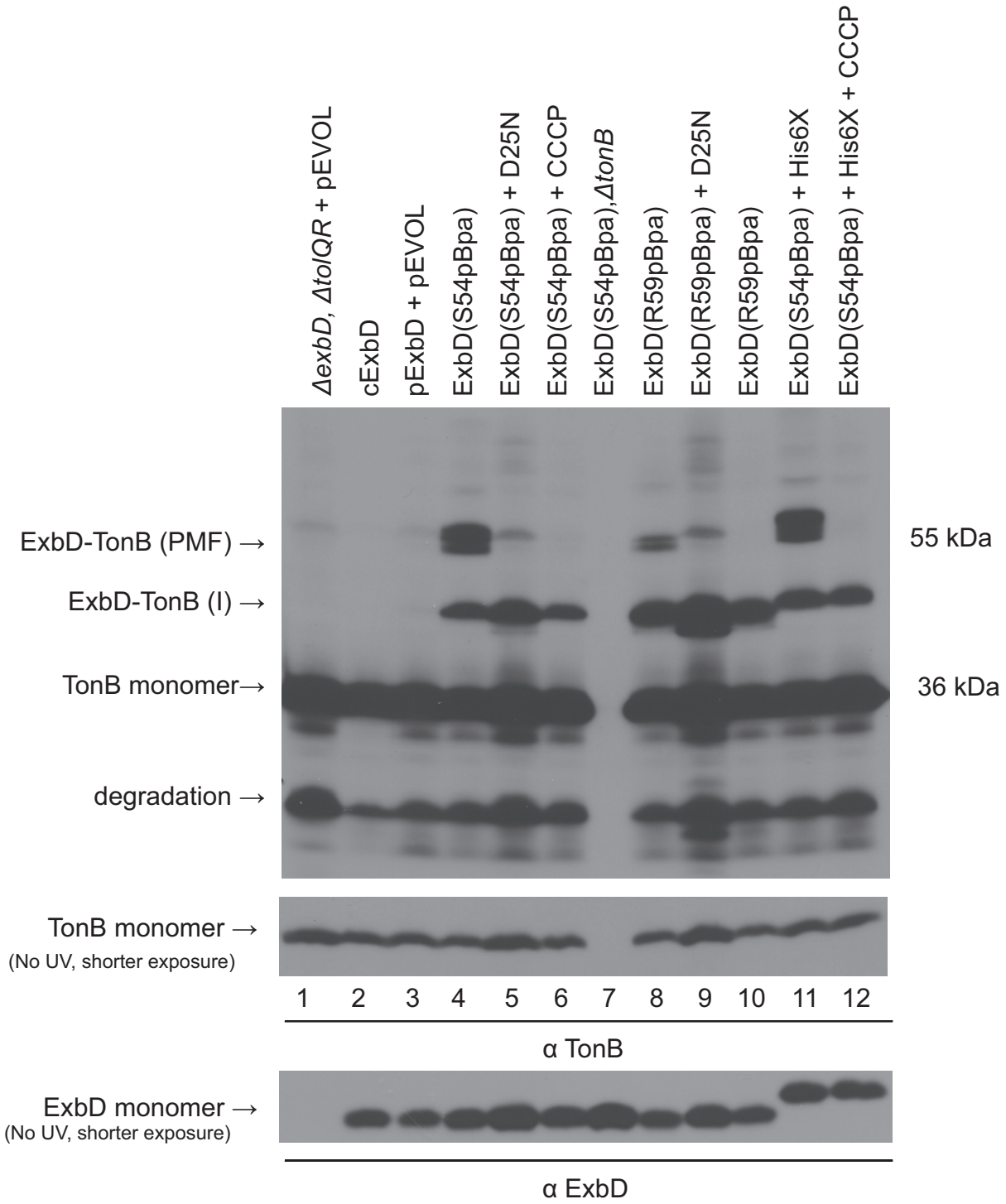


**Figure 3: Both ExbD-TonB PMF-dependent and PMF-independent complexes can be identified by *in vivo* photo-cross-linking.** Plasmid-encoded ExbD (pBpa) substitutions were co-expressed with pEVOL in strain RA1045 (Δ*exbD*, Δ*tolQR*). At mid-exponential phase, strains were subjected to UV irradiation for photo-cross-linking as described in Materials and

767 Methods. Equivalent numbers of cells were precipitated with TCA and the ExbD-TonB
768 complexes were visualized on immunoblots of 13% SDS-polyacrylamide gels by anti-TonB
769 monoclonal antibodies. cExbD designates chromosomally expressed ExbD from the wild-type
770 strain, W3110. The parent plasmid strain pExbD (pKP999) and all ExbD (pBpa) substitutions
771 were expressed in RA1045 (Δ*exbD*, Δ*tolQR*), except for ExbD (S54pBpa) Δ*tonB*, which was
772 expressed in KP1509 (Δ*exbD*, Δ*tolQR, ΔtonB*). D25N is a mutation in the ExbD TMD. The
773 protonophore CCCP was added prior to UV exposure. His6X refers to ExbD (S54pBpa) with a
774 C-terminal $His_6$ tag. On the left, positions of a PMF-dependent ExbD-TonB complex [ExbD-
775 TonB (PMF], a PMF-*in*dependent complex [ExbD-TonB (I)], monomeric TonB, and a TonB
776 degradation product are shown. Mass markers are indicated on the right. Steady state ExbD
777 and TonB monomer levels from the same experiment were determined by immunoblot analysis
778 of control samples that were not exposed to UV light (bottom). The plasmid identities and
779 concentrations of propionate for chromosomal expression are listed in Table S1.

780
781
782
783
784
785
786
787
788
789
790
791
792

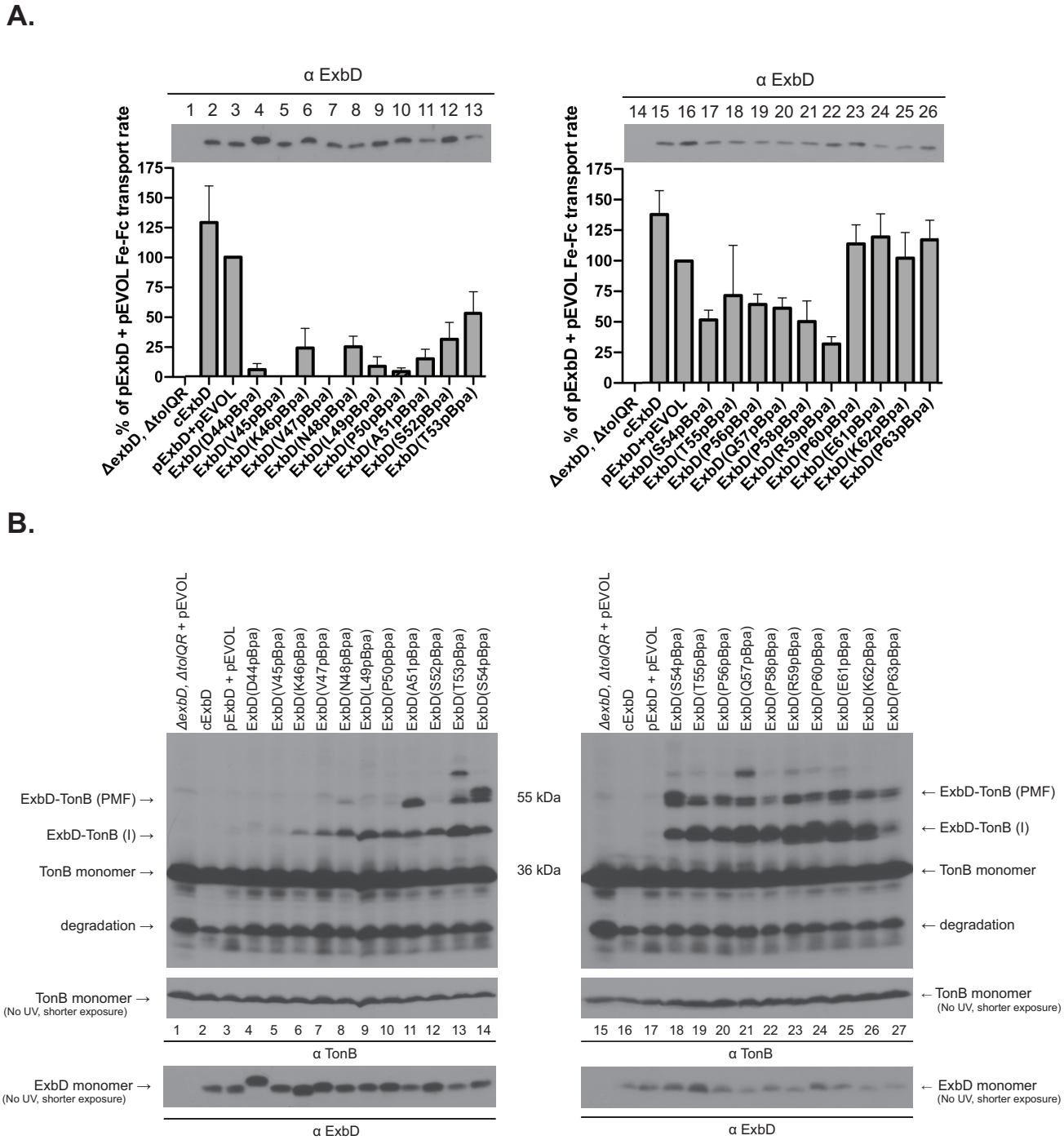


**Figure 4: Virtually all the ExbD (pBpa) substitutions in the ExbD disordered region capture PMF-dependent or PMF-*in*dependent TonB complexes.** (A) Initial rate of $^{55}$Fe-ferrichrome transport for ExbD (pBpa) substitutions at residues 44-54 (left panel) and residues 54-63 (right panel) with the corresponding steady-state expression levels of ExbD proteins at

799 the time of assay above each panel. Plasmid-encoded ExbD pBpa substitutions were co-
800 expressed with plasmid pEVOL in RA1045 (Δ*exbD*, Δ*tolQR*). Strains were grown to mid-
801 exponential phase and assayed as described in Methods and Materials. The percentages of
802 activity were calculated relative to the initial rate for $^{55}$Fe-ferrichrome transport of plasmid-
803 encoded ExbD, pExbD (pKP999). Assays were performed in triplicate and carried out at least
804 twice for each strain. The slopes were determined by a linear regression fit of scintillation
805 counts per minute. The error bars indicate mean ± SEM for a representative triplicate set.
806 cExbD designates chromosomally expressed ExbD from the wild-type strain, W3110. The
807 plasmid identities and concentrations of propionate for chromosomal expression are listed in
808 Table S1. (B) *In vivo* photo-cross-linking of pBpa substitutions for ExbD residues 44-54 (left
809 panel) and residues 54-63 (right panel) on an anti-TonB immunoblot. Note that ExbD S54
810 (pBpa) is included on both immunoblots in lanes 14 and 18 for comparison of levels of
811 expression. On the left and right, positions of a PMF-dependent ExbD-TonB complex [ExbD-
812 TonB (PMF)], a PMF-*in*dependent complex [ExbD-TonB (I)], monomeric TonB, and a TonB
813 degradation product are shown. Mass markers are indicated in the center. The steady-state
814 levels of ExbD and TonB monomers (bottom) from the same experiment were determined by
815 immunoblot analysis of control samples that were not exposed to UV light.

816

817

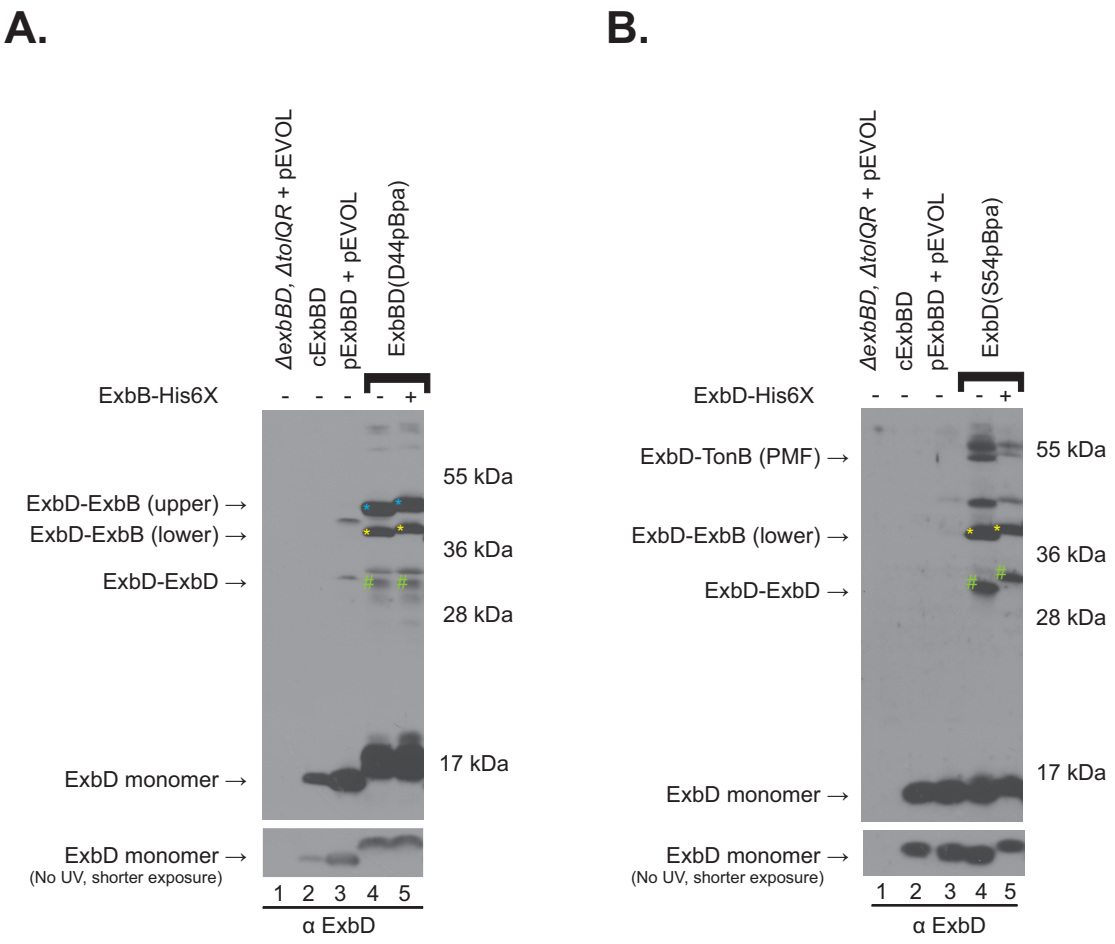


818

819 **Figure 5: Two different ExbD-ExbB complexes and an ExbD homodimer are identified by**
820 ***in vivo* photo-cross-linking**. (A) *In vivo* photo-cross-linking of a representative ExbD photo-
821 cross-linkable mutant, ExbD (D44pBpa), in the presence of ExbB with (+) and without (-) a C-
822 terminal $His_6$ epitope tag (His6X). At mid-exponential phase, strains were subjected to UV
823 irradiation for photo-cross-linking as described in Materials and Methods. Equivalent numbers
824 of cells were precipitated with TCA and the ExbD complexes were visualized on immunoblots
825 of 13% SDS-polyacrylamide gels with anti-ExbD polyclonal antibodies. cExbD designates
826 chromosomally expressed ExbB and ExbD from the wild-type strain, W3110. Plasmid pExbBD
827 (pKP1657) and its corresponding ExbD (D44pBpa) variants were expressed with pEVOL in

828 RA1017 (W3110, *ΔexbBD::kan, ΔtolQRA*). ExbD is overexpressed from plasmid pExbBD and
829 its corresponding ExbD (D44pBpa) variant in the absence of inducer relative to chromosomally
830 ExbD expression under the conditions of this assay. Positions of ExbD-ExbB (upper)—blue
831 asterisk on immunoblot, ExbD-ExbB (lower)—yellow asterisk on immunoblot, likely ExbD-ExbD
832 homodimers–green pound symbol on immunoblot, and ExbD monomer are indicated on the
833 left. pExbBD expressed with pEVOL (lane 3) forms two unidentified complexes that were not
834 ExbD residue-specific (unlabeled). Mass markers are indicated on the right. Steady-state ExbD
835 monomer levels from the same experiment were determined by immunoblot analysis of control
836 samples that were not exposed to UV light. The plasmid identities and concentrations of
837 propionate for chromosomal expression are listed in Table S1. (B) *In vivo* photo-cross-linking
838 of ExbD (S54pBpa), with (+) and without (-) a C-terminal $His_6$ tag (His6X) using the same
839 procedure as in (A). Plasmid pExbD (pKP999) and a corresponding variant, ExbD (S54pBpa)
840 were expressed with pEVOL in RA1045 (Δ*exbD*, Δ*tolQR*). On the left, positions of a PMF-
841 dependent ExbD-TonB complex [ExbD-TonB (PMF], ExbD-ExbB, an ExbD homodimer, and
842 monomeric ExbD are shown. Mass markers are indicated on the right. Steady-state ExbD
843 monomer levels from the same experiment were determined by immunoblot analysis of control
844 samples that were not exposed to UV light (bottom). The plasmid identities and concentrations
845 of propionate for chromosomal expression are listed in Table S1.

846

847

848

849

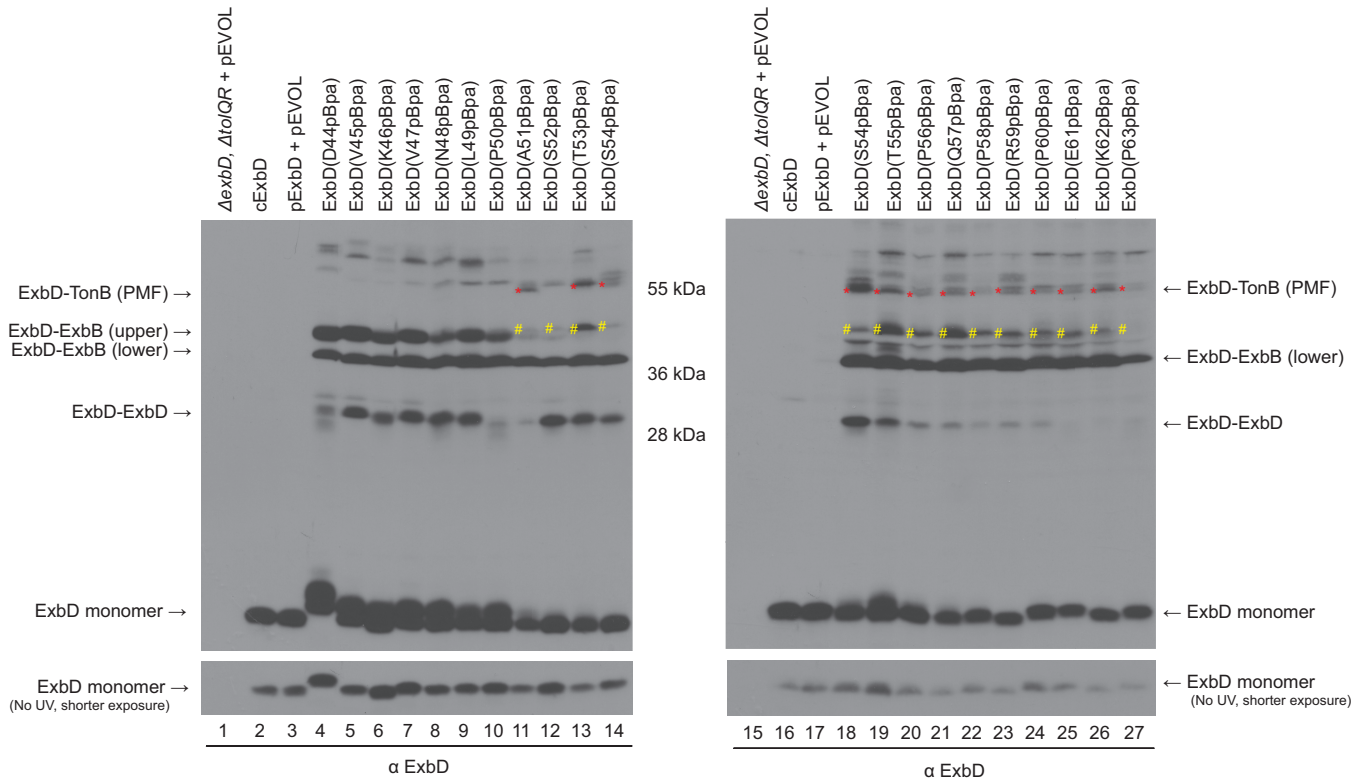


**Figure 6: The majority of pBpa substitutions in the ExbD disordered region capture contacts with ExbB and ExbD.** *In vivo* photo-cross-linking of ExbD pBpa substitutions in residues 44-54 (left panel) and 54-63 (right panel) from Fig. 4 probed with anti-ExbD antibodies. Note that ExbD (S54pBpa) is included on both immunoblots in lanes 14 and 18 for comparison of levels of expression. Strains were grown to mid-exponential phase, at which point photo-cross-linking was performed as described in Materials and Methods. Equivalent numbers of cells were precipitated with TCA and the ExbD-TonB complexes were visualized on immunoblots of 13% SDS-polyacrylamide gels with anti-ExbD polyclonal antibodies. cExbD designates chromosomally expressed ExbD from the wild-type strain, W3110. Plasmid pExbD (pKP999) and its corresponding ExbD pBpa substitutions were expressed in RA1045 (Δ*exbD*, Δ*tolQR*) with plasmid pEVOL. Positions of the PMF-dependent ExbD-TonB complex identified in Fig. 3, ExbD-ExbB (upper) and ExbD-ExbB (lower) from Figure 5A, the ExbD-ExbD from Figure 5B and ExbD monomer are indicated on the right and left. The ExbD-TonB (PMF) is

865 identified by a red asterisk (*). The ExbD-TonB PMF-*in*dependent complex is distinguished
866 from ExbB-ExbD (upper) by a yellow pound symbol (#). Mass standards are in the center. The
867 steady-state ExbD levels from the same experiment were determined by immunoblot analysis
868 of control samples that were not exposed to UV light (bottom). The plasmid identities and
869 concentrations of propionate for chromosomal expression are listed in Table S1.

870

871

872

873

874

875

876

877

878

879

880

881

882

883

# A.

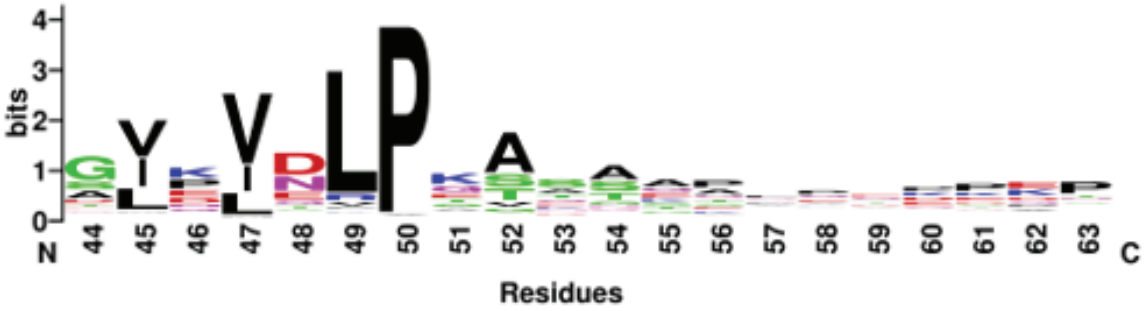


# B.

```
CLUSTAL multiple sequence alignment by MUSCLE (3.8)

ExbD (38) ---APLATVDVKVNLPASTSTPQPRPE------------KPVYLSVKA--------(60)
TolR (36) ---APIITQSVEVDLPDATESQAVSSNDN----------PPVIVEVSG--------(60)
MotB (61) YFRTPLATAVTGGDRISNSESPIPGGGDDYTQSQGEVNKQPNIEELKKRMEQSRLR (116)
```

**Figure 7: The ExbD disordered region contains conserved a ΨXΨXLP motif.** The psi symbol (Ψ) represents a residue with a large aliphatic side chain and X represents any non-hydrophobic residue. (A) A WebLogo image of the ExbD disordered region. The image was generated from an ExbD multiple sequence alignment by HHblits of sequences within an E-value of $e^{-10}$ of *Escherichia coli K-12* strain (NP_417478.1) using the Gremelin.bakerlab program (gremlin.bakerlab.org/). Positions with >75% sequences alignment gaps were removed. (B) A multiple sequence alignment was used to identify potential ΨXΨXLP motifs in ExbD homologs TolR and MotB. A clustal multiple sequence alignment was generated by MUSCLE (3.8) of *Escherichia coli* ExbD (AAA69172.1), TolR (PSM33938.1), and MotB (ACB03086.1). A red box encompasses the *Escherichia coli* K12 ExbD ΨXΨXLP motif

897 containing conserved residues V45, V47, L49 and P50 and shows that these residues are
898 conserved in TolR but not MotB.
899
900
901
902
903
904
905
906
907
908
909
910
911
912
913
914
915

**A.**

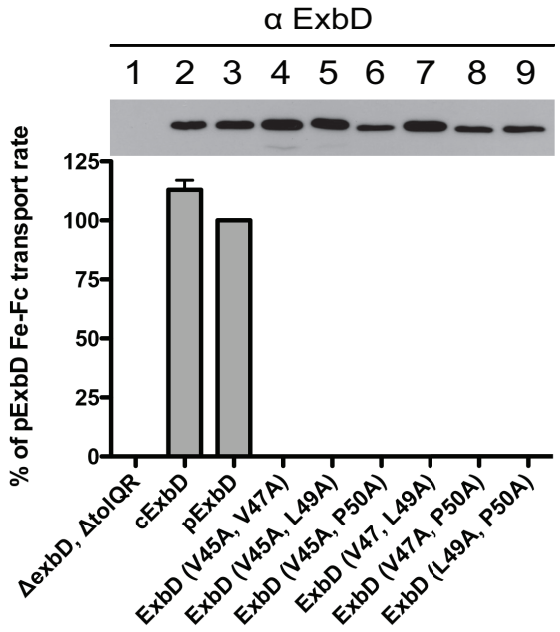


**B.**

| Mutant | Colicin B⁺ | Colicin Ia⁺ | Colicin M⁺ |
|---|---|---|---|
| pExbD | 8, 9, 8 | 8, 8, 8 | 8, 8, 8 |
| ExbD (V45A, V47A) | T, T, T | T, T, T | T, T, T |
| ExbD (V45A, L49A) | T, T, T | T, T, T | T, T, T |
| ExbD (V45A, P50A) | T, T, T | 0*, 0*, 0* | T, T, T |
| ExbD (V47A, L49A) | T, T, T | T, T, T | T, T, T |
| ExbD (V47A, P50A) | T, T, T | T, T, T | T, T, T |
| ExbD (L49A, P50A) | T, T, T | T, T, T | T, T, T |

⁺ T refers to tolerant to undiluted colicin lysate
* 0 refers to hazy clearing in with undiluted colicin

**Figure 8: The synergy of double-Alanine substitutions within the ExbD ΨXΨXLP motif establishes its essentiality for TonB-dependent energy transduction.**

(A) Initial rate of $^{55}$Fe-ferrichrome transport for ExbD variants with the corresponding steady-state expression levels of ExbD proteins at the time of assay above each panel. Strains were grown to mid-exponential phase and assayed as described in Methods and Materials. The percentages of activity were calculated relative to the initial rate for $^{55}$Fe-ferrichrome transport of plasmid-encoded ExbD, pExbD (pKP999). Assays were performed in triplicate and carried out at least twice for each strain. The slopes were determined by a linear regression fit of scintillation counts per minute. The error bars indicate mean ± SEM for a representative triplicate set (above). Steady-state levels of ExbD-specific expression from the transport experiments are indicated above the corresponding bars of the graph below them. cExbD designates chromosomally expressed ExbD from the wild-type strain, W3110. The plasmid identities and concentrations of propionate for chromosomal expression are listed in Table S1.

931 (B) Colicin sensitivity assay. Strains were grown to mid-exponential phase and assayed in
932 triplicate with Colicin B, Colicin Ia, and Colicin M as described in the Material and Methods.
933 pExbD (pKP999) and all ExbD Alanine substitutions were expressed from plasmids in RA1045
934 (Δ*exbD*, Δ*tolQR*). The plasmid identities and concentrations of propionate for chromosomal
935 expression are listed in Table S1. Scoring was reported as the highest 5-fold colicin dilution
936 that produced clearing in three different trials. “T” refers to colicin tolerance (insensitivity) and
937 “0” refers to hazy clearing caused by the undiluted colicin lysate.

938

939

940

941

942

943

944

945

946

947

948

949

950

951

952

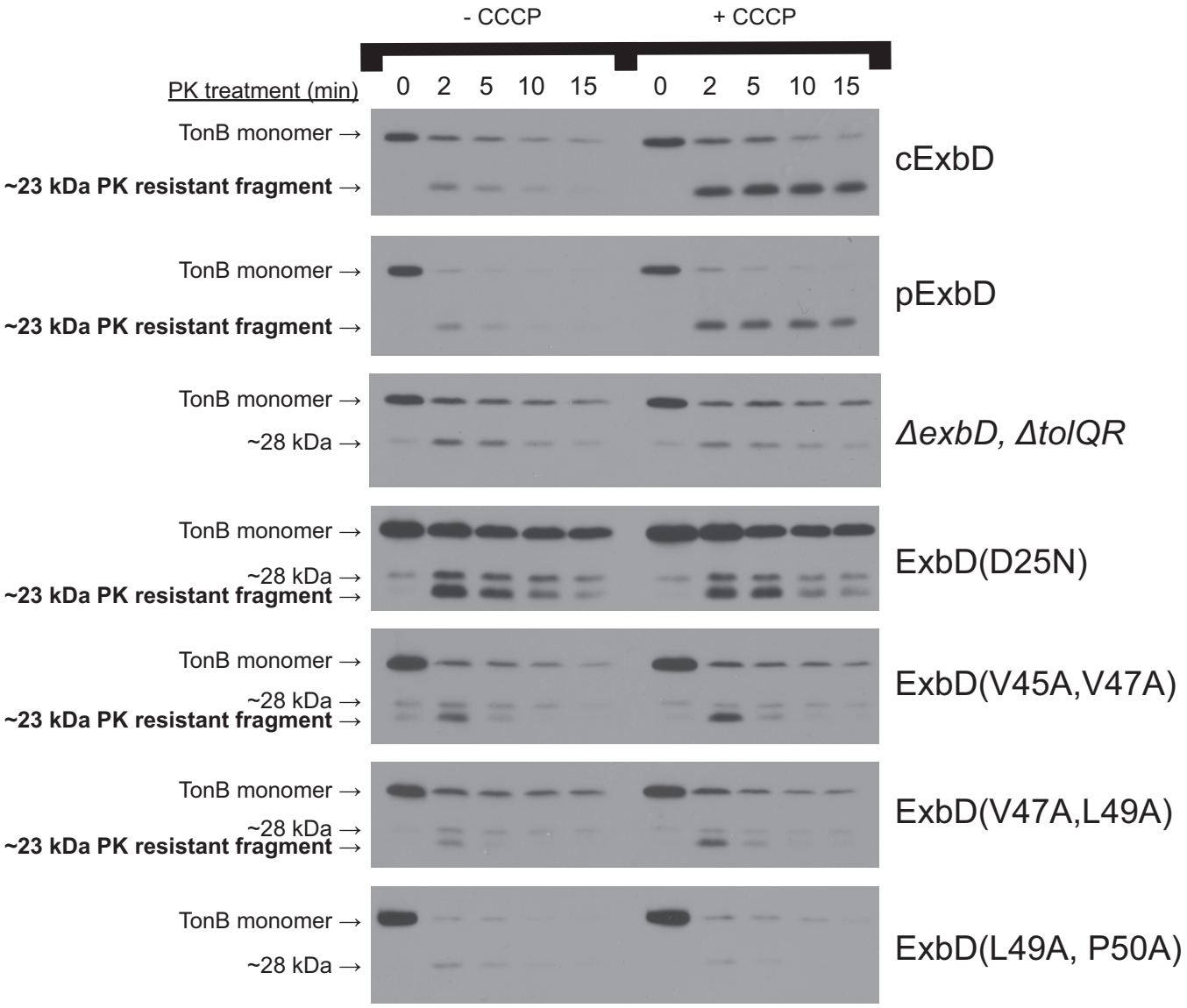
- CCCP
+ CCCP
PK treatment (min)
0 2 5 10 15 0 2 5 10 15
TonB monomer →
~23 kDa PK resistant fragment →
cExbD
TonB monomer →
~23 kDa PK resistant fragment →
pExbD
TonB monomer →
~28 kDa →
ΔexbD, ΔtolQR
TonB monomer →
~28 kDa →
~23 kDa PK resistant fragment →
ExbD(D25N)
TonB monomer →
~28 kDa →
~23 kDa PK resistant fragment →
ExbD(V45A,V47A)
TonB monomer →
~28 kDa →
~23 kDa PK resistant fragment →
ExbD(V47A,L49A)
TonB monomer →
~28 kDa →
ExbD(L49A, P50A)

953

955 **Figure 9: Mutations in the ExbD ΨXΨXLP motif leave TonB stalled at Stage II even when**
956 **PMF is present.** Spheroplasts were generated from W3110 (cExbD), and RA1045 (Δ*exbD*,
957 Δ*tolQR*), as well as RA1045 containing plasmids pKP999 (pExbD), pKP1194 [ExbD (D25N)],
958 pKP2171 [ExbD (V45A, V47A)], pKP2201 [ExbD (V47A, L49A)], and pKP2202 [ExbD (L49A,
959 P50A)] as described in the Materials and Methods. Each spheroplast was treated with
960 proteinase K (PK) for 0 min, 2 min, 5 min, 10 min and 15 min in the presence of DMSO (-
961 CCCP) or CCCP dissolved in DMSO (+CCCP). The samples were visualized on immunoblots
962 of 13% SDS-polyacrylamide gels with anti-TonB monoclonal antibodies. Identities of the
963 various strains assayed are indicated on the left. Positions of TonB monomers, the ~23 kDa
964 PK-resistant TonB fragment indicative of Stage II of TonB energization and the ~28 kDa
965 fragment with no known relevance to any Stage in the TonB energization cycle are on the left
966 (34). The appearance of the ~23 kDa TonB fragment upon lengthy exposure of ExbD (L49A,
967 P50A) samples allowed confident identification of the 28 kDa TonB fragment generated in that
968 strain. The concentrations of propionate for chromosomal expression are listed in Table S1.

969

970

971

972

973

974

975

976

977

978

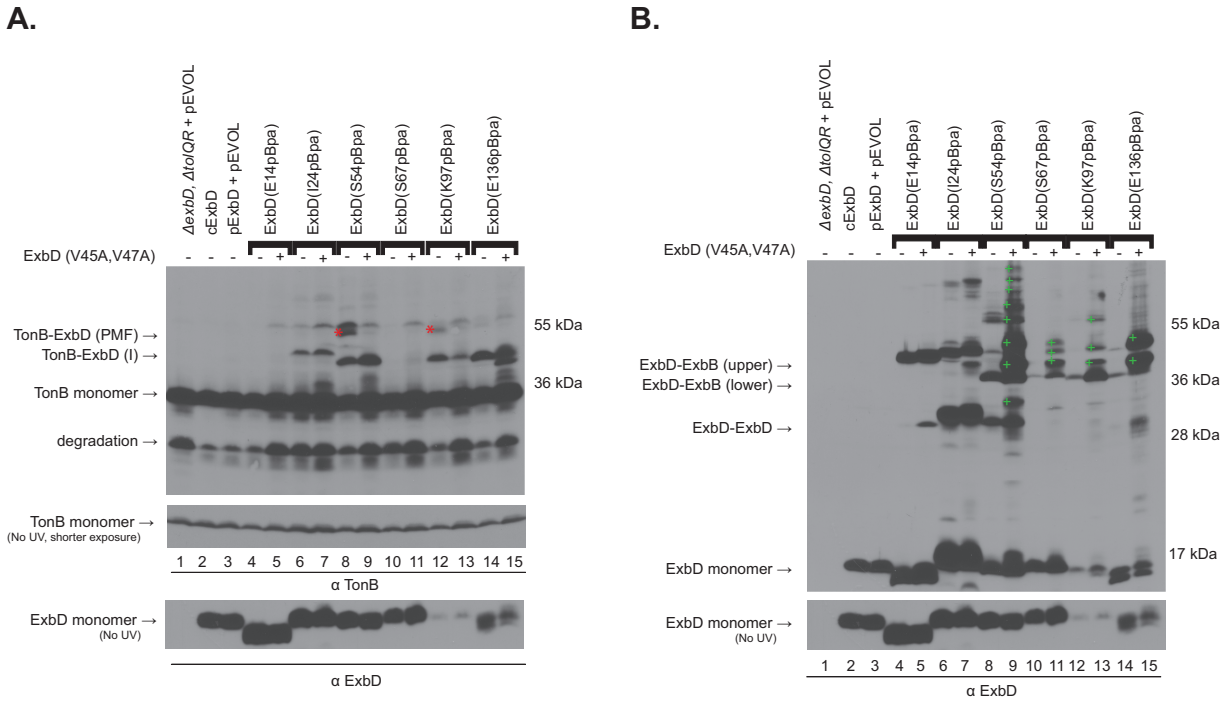


979

980

981 **Figure 10: The N-terminal ExbD ΨXΨXLP motif is required for signal transduction to its**
982 **C-terminus.** *In vivo* photo-cross-linking of ExbD (E14pBpa), ExbD (I24pBpa), ExbD
983 (S54pBpa), ExbD (S67pBpa), ExbD (K97pBpa), and ExbD (E136pBpa) with (+) and without (-)
984 V45A, V47A double Alanine substitutions. Strains were grown to mid-exponential phase, at
985 which point photo-cross-linking was performed as described in Materials and Methods.
986 Equivalent numbers of cells were precipitated with TCA and the samples were visualized on
987 immunoblots of 13% SDS-polyacrylamide gels with either (A) anti-TonB monoclonal antibodies
988 or (B) anti-ExbD polyclonal antibodies. cExbD designates chromosomally expressed ExbD
989 from the wild-type strain, W3110. The parent plasmid pExbD (pKP999) and corresponding
990 ExbD variants were co-expressed with plasmid pEVOL in RA1045 (Δ*exbD*, Δ*tolQR*). (A) On
991 the left, positions of a PMF-dependent ExbD-TonB complex [ExbD-TonB (PMF)—red asterisk],

992 a PMF-*in*dependent complex [ExbD-TonB (I)], monomeric TonB, and a TonB degradation
993 product are shown (See Fig. 3). Mass markers are indicated on the right. Steady state ExbD
994 and TonB monomer levels from the same experiment were determined by immunoblot analysis
995 of control samples that were not exposed to UV light (bottom). (B) On the left, positions of
996 ExbD-ExbB (upper) and ExbD-ExbB (lower) (see Figure 5A), the ExbD-ExbD homodimer (see
997 Figure 5B) and ExbD monomer are shown. Unidentified complexes trapped by the ExbD pBpa
998 variants containing V45A,V47A are indicated on the immunoblot by a green (+) symbol. Mass
999 markers are indicated on the right. Steady-state ExbD levels from the same experiment were
1000 determined by immunoblot analysis of control samples that were not exposed to UV light
1001 (bottom). The plasmid identities and concentrations of propionate for chromosomal expression
1002 are listed in Table S1.

1003

1004

1005

1006

1007

1008

1009

1010

1011

1012

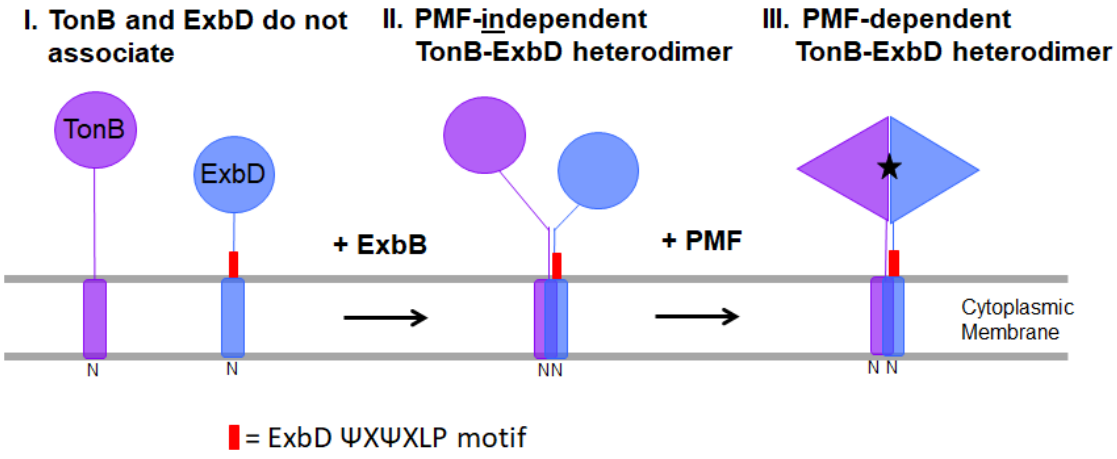


1013

1014

1015 **Figure 11: The ExbD ΨXΨXLP motif is required for TonB to respond to PMF in vivo.**

1016 Model for the initial Stages of TonB energization [adapted from ref (24) with permission from

1017 the publisher]. This updated model covers the behavior of a single TonB. For an expanded

1018 model that accounts for behavior of TonB homodimers in the same context, see (24)]. In

1019 Stage I, ExbD and TonB do not interact, although both are stabilized by ExbB homotetramers

1020 (not shown). In Stage II, the ExbD TMD, adjacent ΨXΨXLP motif (red box), and the rest of the

1021 ExbD disordered domain directly interact with TonB in a PMF-*in*dependent manner, indicating

1022 their in vivo proximity. The C-termini of ExbD and TonB do not interact. In Stage III, the

1023 conformational relationship between ExbD and TonB changes in response to PMF such that

1024 TonB is correctly configured by ExbD for energy transmission to a TBDT, a transition for which

1025 the ExbD ΨXΨXLP motif is required. Stage IV (not shown) is interaction of TonB with a TBDT.

1026 TonB is then recycled back to Stage I.

1027 # REFERENCES:


1028 1. **Sheldon JR, Laakso HA, Heinrichs DE.** 2016. Iron Acquisition Strategies of Bacterial Pathogens. Microbiol
1029 Spectr **4**.

1030 2. **Schauer K, Rodionov DA, de Reuse H.** 2008. New substrates for TonB-dependent transport: do we only
1031 see the 'tip of the iceberg'? Trends Biochem Sci **33:**330-338.

1032 3. **Miethke M, Marahiel MA.** 2007. Siderophore-based iron acquisition and pathogen control. Microbiol
1033 Mol Biol Rev **71:**413-451.

1034 4. **Noinaj N, Guillier M, Barnard TJ, Buchanan SK.** 2010. TonB-dependent transporters: regulation,
1035 structure, and function. Annu Rev Microbiol **64:**43-60.

1036 5. **Hickman SJ, Cooper REM, Bellucci L, Paci E, Brockwell DJ.** 2017. Gating of TonB-dependent transporters
1037 by substrate-specific forced remodelling. Nat Commun **8:**14804.

1038 6. **Larsen RA, Thomas MG, Postle K.** 1999. Protonmotive force, ExbB and ligand-bound FepA drive
1039 conformational changes in TonB. Mol. Microbiol. **31:**1809-1824.

1040 7. **Gresock MG, Postle K.** 2017. Going Outside the TonB Box: Identification of Novel FepA-TonB
1041 Interactions In Vivo. J Bacteriol **199**.

1042 8. **Ferguson AD, Amezcua CA, Halabi NM, Chelliah Y, Rosen MK, Ranganathan R, Deisenhofer J.** 2007.
1043 Signal transduction pathway of TonB-dependent transporters. Proc Natl Acad Sci U S A **104:**513-518.

1044 9. **Moeck GS, Coulton JW, Postle K.** 1997. Cell envelope signaling in *Escherichia coli.* Ligand binding to the
1045 ferrichrome-iron receptor FhuA promotes interaction with the energy-transducing protein TonB. J. Biol.
1046 Chem. **272:**28391-28397.

1047 10. **Cornelissen CN, Anderson JE, Sparling PF.** 1997. Energy-dependent changes in the gonococcal
1048 transferrin receptor. Mol. Microbiol. **26:**25-35.

1049 11. **Krewulak KD, Vogel HJ.** 2011. TonB or not TonB: is that the question? Biochemistry and cell biology =
1050 Biochimie et biologie cellulaire **89:**87-97.

1051 12. **Bradbeer C.** 1993. The proton motive force drives the outer membrane transport of cobalamin in
1052 *Escherichia coli*. J. Bacteriol. **175:**3146-3150.
1053 13. **Higgs PI, Larsen RA, Postle K.** 2002. Quantitation of known components of the *Escherichia coli* TonB-
1054 dependent energy transduction system: TonB, ExbB, ExbD, and FepA. Mol. Microbiol. **44:**271-281.
1055 14. **Kampfenkel K, Braun V.** 1993. Topology of the ExbB protein in the cytoplasmic membrane of *Escherichia*
1056 *coli*. J. Biol. Chem. **268:**6050-6057.
1057 15. **Baker KR, Postle K.** 2013. Mutations in *Escherichia coli* ExbB transmembrane domains identify
1058 scaffolding and signal transduction functions and exclude participation in a proton pathway. J Bacteriol
1059 **195:**2898-2911.
1060 16. **Roof SK, Allard JD, Bertrand KP, Postle K.** 1991. Analysis of *Escherichia coli* TonB membrane topology by
1061 use of PhoA fusions. J. Bacteriol. **173:**5554-5557.
1062 17. **Kampfenkel K, Braun V.** 1992. Membrane topology of the *Escherichia coli* ExbD protein. J. Bacteriol.
1063 **174:**5485-5487.
1064 18. **Eick-Helmerich K, Braun V.** 1989. Import of biopolymers into Escherichia coli: nucleotide sequences of
1065 the *exbB* and *exbD* genes are homologous to those of the *tolQ* and *tolR* genes, respectively. J Bacteriol
1066 **171:**5117-5126.
1067 19. **Gerding MA, Ogata Y, Pecora ND, Niki H, de Boer PA.** 2007. The trans-envelope Tol-Pal complex is part
1068 of the cell division machinery and required for proper outer-membrane invagination during cell
1069 constriction in E. coli. Molecular microbiology **63:**1008-1025.
1070 20. **Cascales E, Lloubes R, Sturgis JN.** 2001. The TolQ-TolR proteins energize TolA and share homologies with
1071 the flagellar motor proteins MotA-MotB. Mol Microbiol **42:**795-807.
1072 21. **Brinkman KK, Larsen RA.** 2008. Interactions of the energy transducer TonB with noncognate energy-
1073 harvesting complexes. J Bacteriol **190:**421-427.
1074 22. **Kadner RJ, Heller KJ.** 1995. Mutual inhibition of cobalamin and siderophore uptake systems suggests
1075 their competition for TonB function. J Bacteriol **177:**4829-4835.

1076 23. **Kaserer WA, Jiang X, Xiao Q, Scott DC, Bauler M, Copeland D, Newton SM, Klebba PE.** 2008. Insight
1077 from TonB hybrid proteins into the mechanism of iron transport through the outer membrane. J
1078 Bacteriol **190:**4001-4016.
1079 24. **Gresock MG, Kastead KA, Postle K.** 2015. From Homodimer to Heterodimer and Back: Elucidating the
1080 TonB Energy Transduction Cycle. J Bacteriol **197:**3433-3445.
1081 25. **Shultis DD, Purdy MD, Banchs CN, Wiener MC.** 2006. Outer membrane active transport: structure of the
1082 BtuB:TonB complex. Science (New York, N.Y **312:**1396-1399.
1083 26. **Postle K, Kastead KA, Gresock MG, Ghosh J, Swayne CD.** 2010. The TonB dimeric crystal structures do
1084 not exist *in vivo*. mBio **1**.
1085 27. **Pawelek PD, Croteau N, Ng-Thow-Hing C, Khursigara CM, Moiseeva N, Allaire M, Coulton JW.** 2006.
1086 Structure of TonB in complex with FhuA, *E. coli* outer membrane receptor. Science (New York, N.Y
1087 **312:**1399-1402.
1088 28. **Gresock MG, Savenkova MI, Larsen RA, Ollis AA, Postle K.** 2011. Death of the TonB shuttle hypothesis.
1089 Frontiers in microbiology **2:**206.
1090 29. **Ollis AA, Manning M, Held KG, Postle K.** 2009. Cytoplasmic membrane protonmotive force energizes
1091 periplasmic interactions between ExbD and TonB. Mol Microbiol **73:**466-481.
1092 30. **Jana B, Manning M, Postle K.** 2011. Mutations in the ExbB cytoplasmic carboxy terminus prevent
1093 energy-dependent interaction between the TonB and ExbD periplasmic domains. J Bacteriol **193:**5649-
1094 5657.
1095 31. **Skare JT, Postle K.** 1991. Evidence for a TonB-dependent energy transduction complex in *Escherichia*
1096 *coli*. Mol Microbiol **5:**2883-2890.
1097 32. **Held KG, Postle K.** 2002. ExbB and ExbD do not function independently in TonB-dependent energy
1098 transduction. J Bacteriol **184:**5170-5173.

1099 33. **Fischer E, Günter K, Braun V.** 1989. Involvement of ExbB and TonB in transport across the outer
1100 membrane of *Escherichia coli*: phenotypic complementation of *exb* mutants by overexpressed *tonB* and
1101 physical stabilization of TonB by ExbB. J. Bacteriol. **171:**5127-5134.
1102 34. **Ollis AA, Postle K.** 2012. ExbD mutants define initial stages in TonB energization. J Mol Biol **415:**237-247.
1103 35. **Ollis AA, Kumar A, Postle K.** 2012. The ExbD periplasmic domain contains distinct functional regions for
1104 two stages in TonB energization. J. Bacteriol. **194:**3069-3077.
1105 36. **Swayne C, Postle K.** 2011. Taking the *Escherichia coli* TonB transmembrane domain "Offline"? Non-
1106 protonatable Asn substitutes fully for TonB His20. J Bacteriol **193:**3693-3701.
1107 37. **Garcia-Herrero A, Peacock RS, Howard SP, Vogel HJ.** 2007. The solution structure of the periplasmic
1108 domain of the TonB system ExbD protein reveals an unexpected structural homology with siderophore-
1109 binding proteins. Mol Microbiol **66:**872-889.
1110 38. **Ollis AA, Postle K.** 2011. The same periplasmic ExbD residues mediate *in vivo* interactions between ExbD
1111 homodimers and ExbD-TonB heterodimers. J Bacteriol **193:**6852-6863.
1112 39. **Ollis AA, Postle K.** 2012. Identification of functionally important TonB-ExbD periplasmic domain
1113 interactions *in vivo*. J. Bacteriol. **194:**3078-3087.
1114 40. **Postle K.** 2007. TonB system, *in vivo* assays and characterization. Methods in Enzymology **422:**245-269.
1115 41. **Takatsuka Y, Nikaido H.** 2009. Covalently linked trimer of the AcrB multidrug efflux pump provides
1116 support for the functional rotating mechanism. J Bacteriol **191:**1729-1737.
1117 42. **Bulathsinghala CM, Jana B, Baker KR, Postle K.** 2013. ExbB cytoplasmic loop deletions cause immediate,
1118 proton motive force-independent growth arrest. J Bacteriol **195:**4580-4591.
1119 43. **Braun V, Herrmann C.** 1993. Evolutionary relationship of uptake systems for biopolymers in *Escherichia*
1120 *coli*: cross-complementation between the TonB-ExbB-ExbD and the TolA-TolQ-TolR proteins. Mol
1121 Microbiol **8:**261-268.
1122 44. **Dyson HJ, Wright PE.** 2019. Perspective: the essential role of NMR in the discovery and characterization
1123 of intrinsically disordered proteins. J Biomol NMR.

1124 45. **Young TS, Ahmad I, Yin JA, Schultz PG.** 2010. An enhanced system for unnatural amino acid
1125 mutagenesis in E. coli. J Mol Biol **395:**361-374.
1126 46. **Dorman G, Prestwich GD.** 1994. Benzophenone photophores in biochemistry. Biochemistry **33:**5661-
1127 5673.
1128 47. **Braun V, Gaisser S, Herrmann C, Kampfenkel K, Killman H, Traub I.** 1996. Energy-coupled transport
1129 across the outer membrane of *Escherichia coli*: ExbB binds ExbD and TonB *in vitro*, and leucine 132 in
1130 the periplasmic region and aspartate 25 in the transmembrane region are important for ExbD activity. J.
1131 Bacteriol. **178:**2836-2845.
1132 48. **Metz B, Kersten GF, Hoogerhout P, Brugghe HF, Timmermans HA, de Jong A, Meiring H, ten Hove J,**
1133 **Hennink WE, Crommelin DJ, Jiskoot W.** 2004. Identification of formaldehyde-induced modifications in
1134 proteins: reactions with model peptides. J Biol Chem **279:**6235-6243.
1135 49. **Sverzhinsky A, Chung JW, Deme JC, Fabre L, Levey KT, Plesa M, Carter DM, Lypaczewski P, Coulton JW.**
1136 2015. Membrane Protein Complex ExbB4-ExbD1-TonB1 from Escherichia coli Demonstrates
1137 Conformational Plasticity. Journal of bacteriology.
1138 50. **Braun V.** 1989. The structurally related *exbB* and *tolQ* genes are interchangeable in conferring *tonB*-
1139 dependent colicin, bacteriophage, and albomycin sensitivity. J. Bacteriol. **171:**6387-6390.
1140 51. **Larsen RA, Chen GJ, Postle K.** 2003. Performance of standard phenotypic assays for TonB activity, as
1141 evaluated by varying the level of functional, wild-type TonB. J Bacteriol **185:**4699-4706.
1142 52. **Cascales E, Buchanan SK, Duché D, Kleanthous C, Lloubes R, Postle K, Riley M, Slatin S, Cavard D.** 2007.
1143 Colicin Biology. Micro. Mol. Biol. Rev. **71:**158-229.
1144 53. **van der Lee R, Buljan M, Lang B, Weatheritt RJ, Daughdrill GW, Dunker AK, Fuxreiter M, Gough J,**
1145 **Gsponer J, Jones DT, Kim PM, Kriwacki RW, Oldfield CJ, Pappu RV, Tompa P, Uversky VN, Wright PE,**
1146 **Babu MM.** 2014. Classification of intrinsically disordered regions and proteins. Chem Rev **114:**6589-
1147 6631.

1148 54. **Krojer T, Sawa J, Schafer E, Saibil HR, Ehrmann M, Clausen T.** 2008. Structural basis for the regulated
1149 protease and chaperone function of DegP. Nature **453:**885-890.
1150 55. **Jiang J, Zhang X, Chen Y, Wu Y, Zhou ZH, Chang Z, Sui SF.** 2008. Activation of DegP chaperone-protease
1151 via formation of large cage-like oligomers upon binding to substrate proteins. Proc Natl Acad Sci U S A
1152 **105:**11939-11944.
1153 56. **Larsen RA, Deckert GE, Kastead KA, Devanathan S, Keller KL, Postle K.** 2007. His20 provides the sole
1154 functionally significant side chain in the essential TonB transmembrane domain. J Bacteriol **189:**2825-
1155 2833.
1156 57. **Skare JT, Roof SK, Postle K.** 1989. A mutation in the amino terminus of a hybrid TrpC-TonB protein
1157 relieves overproduction lethality and results in cytoplasmic accumulation. *J. Bacteriol.* **171:**4442-4447.
1158 58. **Larsen RA, Letain TE, Postle K.** 2003. *In vivo* evidence of TonB shuttling between the cytoplasmic and
1159 outer membrane in *Escherichia coli*. Mol Microbiol **49:**211-218.
1160 59. **Larsen RA, Wood GE, Postle K.** 1993. The conserved proline-rich motif is not essential for energy
1161 transduction by *Escherichia coli* TonB protein. Mol Microbiol **10:**943-953.
1162 60. **Vakharia-Rao H, Kastead KA, Savenkova MI, Bulathsinghala CM, Postle K.** 2007. Deletion and
1163 substitution analysis of the *Escherichia coli* TonB Q160 region. J Bacteriol **189:**4662-4670.
1164 61. **Lee GF, Hazelbauer GL.** 1995. Quantitative approaches to utilizing mutational analysis and disulfide
1165 crosslinking for modeling a transmembrane domain. Protein Science **4:**1100-1107.
1166 62. **Sverzhinsky A, Fabre L, Cottreau AL, Biot-Pelletier DM, Khalil S, Bostina M, Rouiller I, Coulton JW.**
1167 2014. Coordinated rearrangements between cytoplasmic and periplasmic domains of the membrane
1168 protein complex ExbB-ExbD of *Escherichia coli*. Structure **22:**791-797.
1169 63. **Lazzaroni JC, Vianney A, Popot JL, Benedetti H, Samatey F, Lazdunski C, Portalier R, Geli V.** 1995.
1170 Transmembrane alpha-helix interactions are required for the functional assembly of the *Escherichia coli*
1171 Tol complex. Journal of Molecular Biology **246:**1-7.

1172 64. **Maki-Yonekura S, Matsuoka R, Yamashita Y, Shimizu H, Tanaka M, Iwabuki F, Yonekura K.** 2018.
1173 Hexameric and pentameric complexes of the ExbBD energizer in the Ton system. Elife **7**.
1174 65. **Celia H, Noinaj N, Zakharov SD, Bordignon E, Botos I, Santamaria M, Barnard TJ, Cramer WA, Lloubes**
1175 **R, Buchanan SK.** 2016. Structural insight into the role of the Ton complex in energy transduction. Nature
1176 **538:**60-65.
1177 66. **Pramanik A, Hauf W, Hoffmann J, Cernescu M, Brutschy B, Braun V.** 2011. Oligomeric Structure of ExbB
1178 and ExbB-ExbD Isolated from *Escherichia coli* as Revealed by LILBID-Mass Spectrometry. Biochemistry
1179 **epub**.
1180 67. **Celia H, Botos I, Ni X, Fox T, De Val N, Lloubes R, Jiang J, Buchanan SK.** 2019. Cryo-EM structure of the
1181 bacterial Ton motor subcomplex ExbB-ExbD provides information on structure and stoichiometry.
1182 Commun Biol **2:**358.
1183 68. **Larsen RA, Thomas MT, Wood GE, Postle K.** 1994. Partial suppression of an *Escherichia coli* TonB
1184 transmembrane domain mutation (ΔV17) by a missense mutation in ExbB. Mol. Microbiol. **13:**627-640.
1185 69. **Laemmli UK.** 1970. Cleavage of structural proteins during the assembly of the head of bacteriophage
1186 T4. Nature **227:**680-685.
1187 70. **Larsen RA, Myers PS, Skare JT, Seachord CL, Darveau RP, Postle K.** 1996. Identification of TonB
1188 homologs in the family *Enterobacteriaceae* and evidence for conservation of TonB-dependent energy
1189 transduction complexes. J. Bacteriol. **178:**1363-1373.
1190 71. **Newton SM, Igo JD, Scott DC, Klebba PE.** 1999. Effect of loop deletions on the binding and transport of
1191 ferric enterobactin by FepA. Mol Microbiol **32:**1153-1165.

1192

1193 # SUPPLEMENTAL INFORMATION

1194 ## Table S1, Kopp and Postle:

| **Strain** | **Genotype** | | **Reference** |
|---|---|---|---|
| W3110 | F− IN(*rrnD-rrnE*)1 | | [1] |
| KP1270 | W3110, *aroB* | | [2] |
| KP1509 | W3110 *ΔexbD ΔtolQR, ΔtonB::kan* | | [5] |
| KP1526 | W3110, *ΔexbD, ΔtolQR, aroB* | | Present Study |
| RA1017 | W3110, *ΔexbBD::kan, ΔtolQRA* | | [4] |
| RA1045 | W3110, *ΔexbD, ΔtolQR* | | [3] |
| **Plasmid** | **Genotype or Phenotype** | **[a]Propionate Induction Concentration** | **References** |
| pEVOL-BpF | tRNA synthetase and tRNA for pBpa insertion, cam$^r$ | N/A | [6] |
| pKP999 | *exbD* in pPro24, amp$^r$ | 0.5 mM | [5] |
| pKP1657 | *exbBD* in pPro24, amp$^r$ | 0 mM | Present study |
| pKP1064 | ExbD (D25N) | 0 mM | [5] |
| pKP2073 | ExbD (44-48Ala) | 0.25 mM | Present study |
| pKP2077 | ExbD (49-53Ala) | 0.5 mM | Present study |
| pKP2153 | ExbD (54-58Ala) | 0.75 mM | Present study |
| pKP2180 | ExbD (59-63Ala) | 20 mM | Present study |
| pKP2140 | ExbD (D44A) | 0.25 mM | Present study |
| pKP2141 | ExbD (V45A) | 2.5 mM | Present study |
| pKP2142 | ExbD (K46A) | 0 mM | Present study |
| pKP2143 | ExbD (V47A) | 1 mM | Present study |
| pKP2144 | ExbD (N48A) | 0.25 mM | Present study |
| pKP2145 | ExbD (L49A) | 0.25 mM | Present study |

| | | | |
|---|---|---|---|
| pKP2154 | ExbD (P50A) | 0 mM | Present study |
| pKP2152 | ExbD (S52A) | 0.25 mM | Present study |
| pKP2146 | ExbD (T53A) | 0.25 mM | Present study |
| pKP2007 | ExbD (D44Am) | 0 mM | Present study |
| pKP2133 | ExbD (V45Am) | 0 mM | Present study |
| pKP2017 | ExbD (K46Am) | 0 mM | Present study |
| pKP2131 | ExbD (V47Am) | 0.5 mM | Present study |
| pKP2018 | ExbD (N48Am) | 2 mM | Present study |
| pKP2147 | ExbD (L49Am) | 0.5 mM | Present study |
| pKP1971 | ExbD (P50Am) | 0 mM | Present study |
| pKP2138 | ExbD (A51Am) | 45 mM | Present study |
| pKP1951 | ExbD (S52Am) | 1 mM | Present study |
| pKP2151 | ExbD (T53Am) | 1 mM | Present study |
| pKP1972 | ExbD (S54Am) | 1 mM | Present study |
| pKP2139 | ExbD (T55Am) | 8 mM | Present study |
| pKP1973 | ExbD (P56Am) | 5 mM | Present study |
| pKP2137 | ExbD (Q57Am) | 10 mM | Present study |
| pKP1974 | ExbD (P58Am) | 5 mM | Present study |
| pKP1898 | ExbD (R59Am) | 5 mM | Present study |
| pKP1975 | ExbD (P60Am) | 8 mM | Present study |
| pKP2027 | ExbD (E61Am) | 10 mM | Present study |
| pKP1949 | ExbD (K62Am) | 8 mM | Present study |
| pKP2136 | ExbD (P63Am) | 7 mM | Present study |
| pKP1926 | ExbD (E14Am) | 4 mM | Present study |

| | | | |
|---|---|---|---|
| pKP2064 | ExbD (I24Am) | 0 mM | Present study |
| pKP2167 | ExbD (S67Am) | 5 mM | Present study |
| pKP2227 | ExbD (K97Am) | 2 mM | Present study |
| pKP1907 | ExbD (E136Am) | 0 mM | Present study |
| pKP2171 | ExbD (V45A, V47A) | 1 mM | Present study |
| pKP2164 | ExbD (V45A, L49A) | 0.5 mM | Present study |
| pKP2182 | ExbD (V45A, P50A) | 0.25 mM | Present study |
| pKP2201 | ExbD (V47A, L49A) | 0.25 mM | Present study |
| pKP2190 | ExbD (V47A, P50A) | 0.25 mM | Present study |
| pKP2202 | ExbD (L49A, P50A) | 0.5 mM | Present study |
| pKP2213 | ExbD (V45A,V47A, E14Am) | 0 mM | Present study |
| pKP2214 | ExbD (V45A,V47A, I24Am) | 0 mM | Present study |
| pKP2161 | ExbD (V45A,V47A, S54Am) | 3 mM | Present study |
| pKP2215 | ExbD (V45A,V47A, S67Am) | 1.5 mM | Present study |
| pKP2228 | ExbD (V45A,V47A, K97Am) | 30 mM | Present study |
| pKP2220 | ExbD (V45A,V47A, E136Am) | 0 mM | Present study |
| pKP2063 | ExbD (S54pBpa, D25N) | 1 mM | Present study |
| pKP1932 | ExbD (R59pBpa, D25N) | 5 mM | Present study |
| pKP2259 | ExbD (S54AM)-His(6x) | 5mM | Present study |
| pKP2295 | ExbB-ExbD (D44Am) | 0 mM | Present study |
| pKP2272 | ExbB-His(6x)-ExbD (D44Am) | 0 mM | Present study |

1196 [a] Propionate concentration required for plasmid induction in RA1045 background strain to
1197 achieve similar W3110 ExbD chromosomal protein levels.

1198

1199 **SUPPLEMENTAL FIGURES Kopp and Postle:**

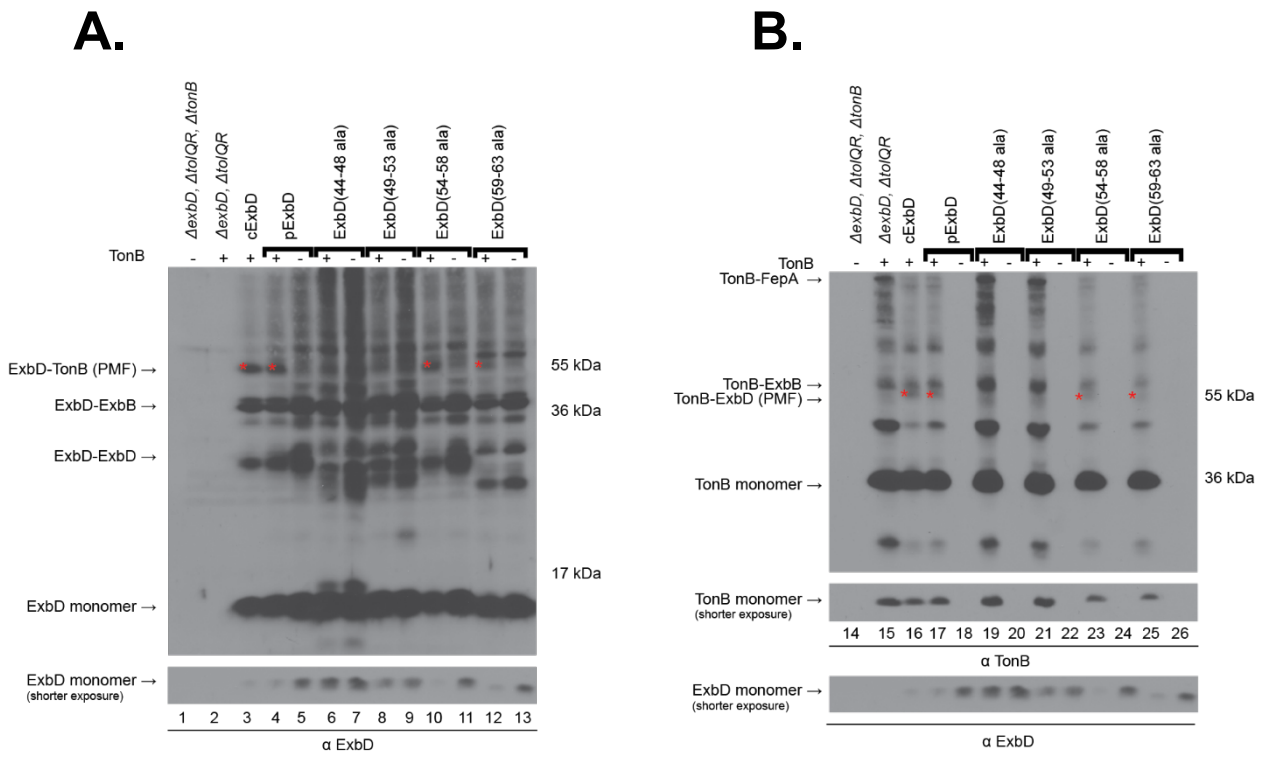


**Figure S1: ExbD (44-48Ala) and ExbD (49-53Ala) fail to form a formaldehyde crosslinked ExbD-TonB PMF-dependent complex.** *In vivo* formaldehyde-cross-linking of block Alanine substitutions in the ExbD disordered region. Strains were grown to mid-exponential phase, at which point formaldehyde-cross-linking was performed as described in Materials and Methods. Equivalent numbers of cells were visualized on immunoblots of 13% SDS-polyacrylamide gels with (A) anti-ExbD polyclonal and (B) anti-TonB monoclonal antibodies. cExbD designates chromosomally expressed ExbD from the wild-type strain, W3110. The parent plasmid, pExbD (pKP999) and its corresponding ExbD block Alanine substitutions were expressed in both RA1045 (Δ*exbD*, Δ*tolQR*) [+] and KP1509 (Δ*exbD*, Δ*tolQR,* Δ*tonB* ) [-]. (A) Positions of the previously characterized formaldehyde cross-linked PMF-dependent ExbD-TonB complex (red asterisk on immunoblot), the ExbD-ExbB complex, the ExbD-ExbD homodimer and ExbD

1214 monomer are shown on the left (5). Mass markers are shown on the right. (B) Positions of the
1215 TonB-FepA complex, the TonB-ExbB complex, the PMF-dependent TonB-ExbD complex and
1216 TonB monomer are shown. Mass markers are shown on the right. Below each immunoblot are
1217 the levels of the corresponding monomer in each sample. The plasmid identities and
1218 concentrations of propionate for chromosomal expression are listed in Table S1.

1219

1220

1221

1222

1223

1224

1225

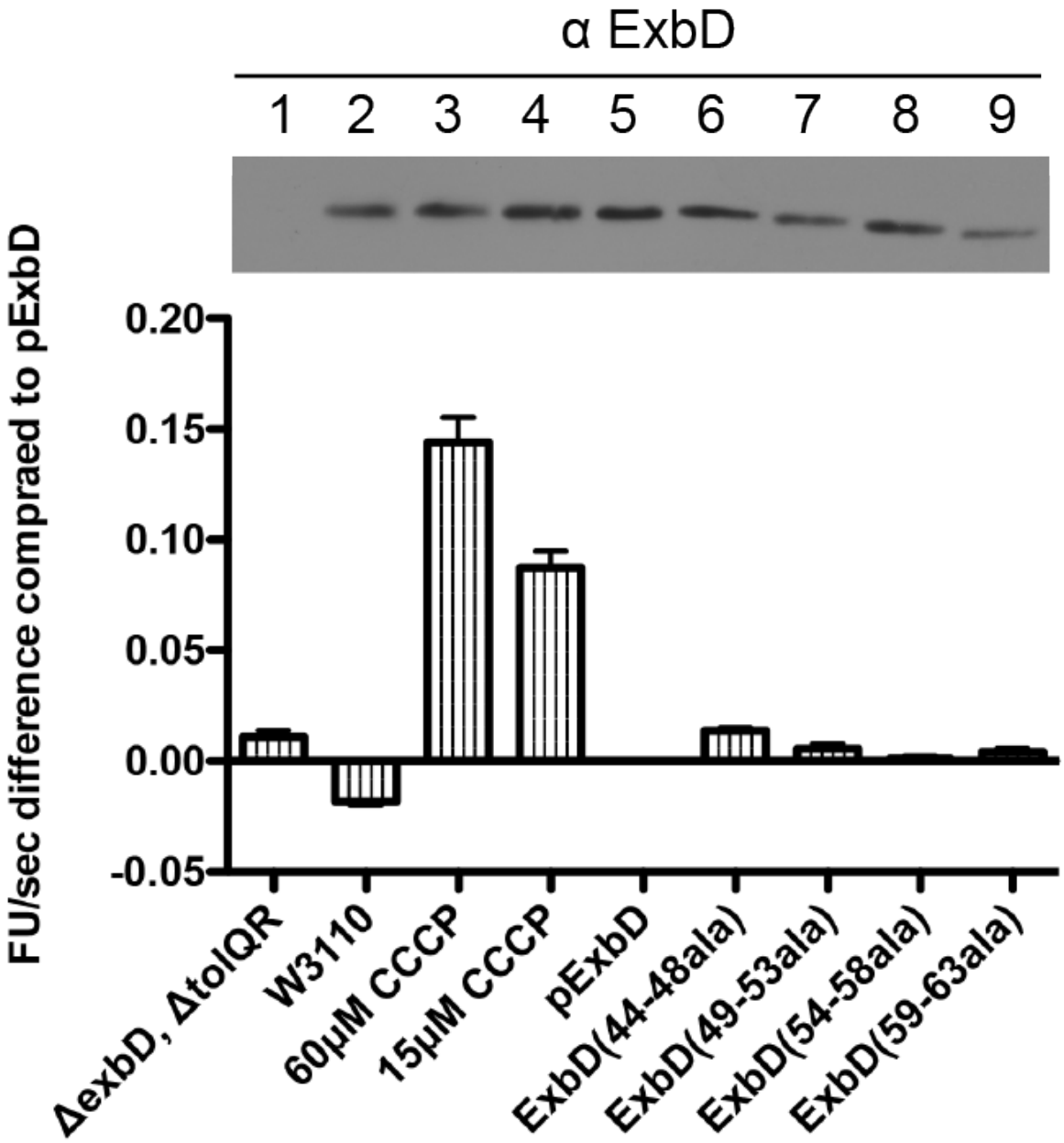


**Figure S2: Failure to form the PMF-dependent ExbD-TonB formaldehyde crosslink is not due to loss of PMF; a small, but significant difference is detected among the block Ala substitutions.** The rate of ethidium bromide (EtBr) accumulation, an indirect assay for loss of PMF, was measured for ExbD block Alanine substitutions as described in the Materials and Methods. Strains were grown to mid-exponential phase and assayed as described in Methods and Materials. (A) The average EtBr accumulation rates (FU/sec) were calculated relative to the rate of plasmid-encoded ExbD, pExbD (pKP999) expressed at chromosomal levels in

1234 RA1045 (Δ*exbD*, Δ*tolQR*). The corresponding steady-state ExbD monomer levels determined
1235 by immunoblot analysis from the experiment from one of the trials are shown above the bar
1236 graph. cExbD designates chromosomally expressed ExbD from the wild-type strain, W3110.
1237 For lanes 3 and 4, W3110 was treated with 60 μM CCCP or 15 μM (as labeled) was prior to
1238 addition of EtBr as described in the Materials and Methods. ExbD Alanine substitutions were
1239 expressed from plasmids in RA1045 (Δ*exbD*, Δ*tolQR*). The plasmids and concentrations of
1240 propionate for chromosomal expression are listed in Table S1. Numbers above the immunoblot
1241 correspond to samples below them starting with (Δ*exbD*, Δ*tolQR*) on the left as #1.

1242

1243

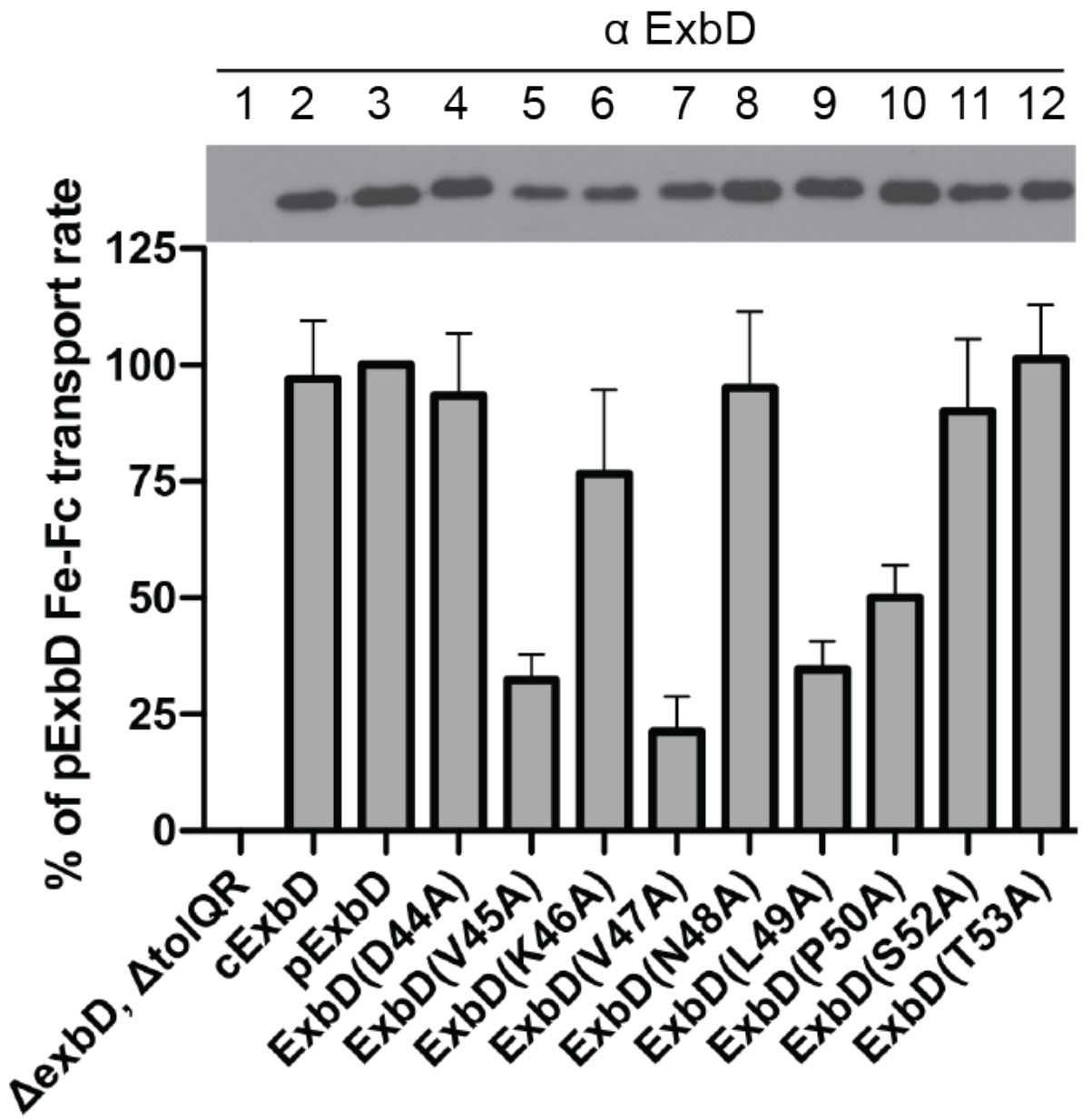


**Figure S3: ExbD residues V45, V47, L49 and P50 are important for TonB System activity.** Plasmid-encoded wild-type ExbD and Alanine substitution mutants were expressed in RA1045 (Δ*exbD*, Δ*tolQR*). Strains were grown to mid-exponential phase and assayed for the initial rate of $^{55}$Fe-ferrichrome transport as described in Methods and Materials. The percentages of activity were calculated relative to the initial rate of plasmid-encoded ExbD, pExbD (pKP999). Assays were performed in triplicate and carried out at least twice for each strain. The slopes

1252 were determined by a linear regression fit of scintillation counts per minute. The error bars
1253 indicate mean ± SEM for a representative triplicate set. cExbD designates chromosomally
1254 expressed ExbD from the wild-type strain, W3110. Plasmid identities and concentrations of
1255 propionate for chromosomal expression are listed in Table S1. The mean percent of the pExbD
1256 $^{55}$Fe-ferrichrome transport rates for ExbD (V45A), ExbD (V47A), ExbD (L49A), and ExbD
1257 (P50A) were 32%, 21%, 34%, and 50% respectively. ExbD residue 51 is naturally an Alanine
1258 in *Escherichia coli* W3110 and is reflected in the pExbD initial rate. Steady-state levels of
1259 ExbD-specific expression from the transport experiments are indicated above the bar graph.

1260
1261
1262
1263
1264
1265
1266
1267
1268
1269
1270
1271
1272
1273
1274
1275
1276
1277

1278 **Supplemental references:**

1279 1. Hill CW, Harnish BW. 1981. Inversions between Ribosomal RNA Genes of *Escherichia*
1280 *coli.* Proc Natl Acad Sci U S A **78**:7069–7072.

1281 2. Larsen RA, Thomas MG, Postle K. 1999. Protonmotive force, ExbB and ligand-bound
1282 FepA Drive Conformational Changes in TonB. Molecular Microbiology **31**:1809–1824.

1283 3. Brinkman KK, Larsen RA. 2008. Interactions of the Energy Transducer TonB with
1284 Noncognate Energy-Harvesting Complexes. J Bacteriol **190**:421–427.

1285 4. Larsen RA, Deckert GE, Kastead KA, Devanathan S, Keller KL, Postle K. 2007. His20
1286 Provides the Sole Functionally Significant Side Chain in the Essential TonB
1287 Transmembrane Domain. J Bacteriol **189:**2825–2833.

1288 5. Ollis AA, Manning M, Held KG, Postle K. 2009. Cytoplasmic Membrane Protonmotive
1289 Force Energizes Periplasmic Interactions between ExbD and TonB. Mol Microbiol
1290 **73**:466–481.

1291 6. Young TS, Ahmad I, Yin JA, Schultz PG. 2010. An Enhanced System for Unnatural Amino
1292 Acid Mutagenesis in *E. coli*. J Mol Biol **395**:361–374.

1293

1294

1295